Université de Montréal

Les biomarqueurs en neuroimagerie des séquelles neurocognitives à long terme chez les survivants de leucémie lymphoblastique aiguë pédiatrique

Par Julie Laniel

Sous la supervision de Sarah Lippé

Département de psychologie

Faculté des Arts et des Sciences

Essai doctoral présenté en vue de l'obtention du grade de Doctorat en psychologie clinique – Option neuropsychologie clinique (D.Psy)

Août, 2023

Table des matières

Résumé

La leucémie lymphoblastique aiguë (LLA) est le cancer pédiatrique le plus commun en Amérique du Nord et les traitements actuels confèrent à la maladie un taux de survie à 5 ans de 85%. Toutefois, suite à la maladie, de nombreux enfants vivent avec les séquelles à long-terme des traitements, incluant des déficits neurocognitifs. Les principaux facteurs de risques associés aux séquelles neurocognitives sont le sexe féminin, un diagnostic en bas âge, et les caractéristiques du protocole de traitement comme l'ajout de la radiothérapie crânienne et l'intensité des doses de chimiothérapie reçues. Cette étude comporte deux objectifs principaux. Le premier consiste à déterminer si le ratio de transfert de magnétisation (MTR), un indicateur de l'intégrité de la myéline, est sensible aux altérations microstructurelles de la substance blanche chez les survivants de la LLA à long-terme, et dans quelle mesure est-il associé aux difficultés cognitives documentées (i.e., fonctions exécutives, mémoire de travail, vitesse de traitement et coordination visuomotrice). Le second objectif est d'étudier l'impact des facteurs de risques sur l'intégrité de la substance blanche . Dans cette étude d'imagerie par transfert de magnétisation, nous comptons 35 survivants de la LLA diagnostiqués en moyenne il y a 18.9 ans (étendue des années écoulées depuis le diagnostic [6.9 – 26.8]) et un groupe contrôle (n=21) sans antécédent de cancer apparié pour l'âge, le sexe et le niveau d'éducation. Les MTRs ont été extraits semi-automatiquement pour l'ensemble de la substance blanche cérébrale et du corps calleux. Les résultats ont révélé des moyennes de MTR plus faibles chez les survivants de la LLA et des associations négatives entre les moyennes de MTR et les doses cumulées des agents de chimiothérapie intrathécale. En conclusion, les résultats suggèrent une détérioration de la myéline chez les survivants de LLA. Cette étude confirme l'intérêt du MTR dans l'examen de la substance blanche.

Mots-clés: leucémie lymphoblastique aiguë, cancer pédiatrique, survivants à long terme, neuropsychologie, séquelles neurocognitives, biomarqueurs, imagerie par résonance magnétique

Abstract

Acute lymphoblastic leukemia (ALL) is the most common pediatric cancer in North America. Research efforts have achieved a five-year survival rate reaching 85% today. However, the number of children experiencing long-term sequelae of treatments, such as neurocognitive deficits, has increased. The main risk factors documented for these neurocognitive deficits are female sex, early age diagnosis and treatment variables such as cranial radiotherapy (CRT), cumulative doses of intravenous (IV) methotrexate (MTX) and intrathecal (IT) chemotherapy (cytarabine, hydrocortisone and MTX). The aims of this study are twofold. The first is to determine if Magnetization Transfer Ratio (MTR), a method assessing myelin integrity, is sensitive to white matter (WM) microstructural alterations in long-term ALL survivors, and whether these are related to the observed cognitive impairments (i.e., impaired executive function, working memory, processing speed and visuomotor coordination). The second is to examine the link between WM integrity and the risk factors. Magnetization transfer imaging was employed to measure WM microstructural integrity in 35 survivors 18.9 years after the ALL onset (years since diagnosis range [6.9 – 26.8]), in addition to 21 age, sex and education level matched controls with no history of cancer. MTRs were semi-automatically extracted from the whole brain WM and the corpus callosum (CC). Results revealed lower MTR means in ALL survivors and negative associations between MTR means and cumulative doses of the intrathecal chemotherapy agents. In conclusion, the results suggest a myelin deterioration in ALL survivors. This study confirms the interest of MTR in WM assessments.

Keywords: Acute lymphoblastic leukemia, Pediatric cancer, Long-term survivors, Neuropsychology, Neurocognitive sequelae, Magnetic resonance imaging

Liste des tableaux

Liste des figures

Liste des abréviations

ALL: Acute lymphoblastic leukemia

ANOVA: Analysis of variance

CC: Corpus callosum

CRT: Cranial radiotherapy

EF: Executive functioning

FDR: False discovery rate

FSIQ: Full-Scale IQ

GAI: General Ability Index

GE: Gradient echo

FSPGR: Magnetization prepared–ultrafast acquisition gradient echo

IR: Inversion recovery

IT: intrathecal

IV: intravenous

MRI: Magnetic resonance imaging

MTR: Magnetization transfer ratio

MT-SPGR: Magnetization transfer spoiled gradient echo

MTX: Methotrexate

PRI: Perceptual Reasoning Index

PSI: Processing Speed Index

TI: Inversion time

TR: Repetition time

SD: Standard deviation

VCI: Verbal Comprehension Index

VOIs: Volumetric regions of interest

WM: White matter

WMI: Working Memory Index

Présentation

Cet essai doctoral est rédigé en anglais sous la forme d'un article de recherche, lequel sera soumis à la revue *Cancers*.

Cumulative Dosage of Intrathecal Chemotherapy Agents Predicts White Matter Integrity in Long-Term Survivors of Acute Lymphoblastic Leukemia: A PETALE study

Author list

Julie Laniel, B.Sc. 1,3
Serge Sultan, Ph.D. 1,3
Daniel Sinnett, Ph.D. 1,4
Caroline Laverdière, M.D. 1,4
Maja Krajinovic, M.D. 1,4,6
Philippe Robaey, M.D, Ph.D. 1,2,5,7
Luc Duong, Ph.D. 1,8
Sarah Lippé, Ph.D. 1,3

Affiliations

1. Azrieli Research Center from CHU Sainte-Justine, Montreal, Quebec, Canada.
2. Children's Hospital of Eastern Ontario (CHEO), Ottawa, Ontario, Canada
3. Université de Montréal, Department of Psychology, Montreal, Quebec, Canada.
4. Université de Montréal, Department of Pediatrics, Montreal, Quebec, Canada
5. Université de Montréal, Department of Psychiatry, Montreal, Quebec, Canada
6. Université de Montréal, Department of Pharmacology, Montreal, Quebec, Canada
7. University of Ottawa, Department of Psychiatry, Ottawa, Ontario, Canada
8. École de technologie supérieure (ETS), Department of software engineering and information technology, Montreal, Quebec, Canada

Sources of funding

Fondation Cole

IRSC

FRQS

Société de recherche sur le cancer

Société canadienne du cancer

Le C17 Council

Pediatric Oncology Group of Ontario (POGO)

Garron Family Cancer Centre du Hospital for Sick Children

Introduction

Acute lymphoblastic leukemia (ALL) remains the most diagnosed pediatric cancer. Fortunately, current treatments allow a 5-year survival rate as high as 80-90%.[1] Treatment regimens are based on a combination of chemotherapeutic agents directed to the central nervous system by intravenous and intrathecal routes, and adjunctive cranial radiotherapy when the risk of relapse is critical. Due to the high risk of cognitive sequelae, cranial radiotherapy is increasingly being replaced by intensified systemic and intrathecal (IT) therapy.[1–3] IT therapy involves delivering medication into the cerebrospinal fluid via lumbar puncture, allowing chemotherapeutic agents to bypass the blood-brain barrier and access the brain. Within the realm of ALL, Cytarabine, methotrexate, and hydrocortisone are common chemotherapeutic agents delivered intrathecally. Cytarabine, an antimetabolite chemotherapy, disrupts cancer cell growth by interfering with DNA synthesis, ultimately inhibiting cell division and promoting cell death. Methotrexate is an antimetabolite that inhibits the enzyme dihydrofolate reductase, which is involved in the production of tetrahydrofolate, a key molecule in the synthesis of nucleic acids. Hydrocortisone is a corticosteroid administered as adjunctive therapy to manage central nervous system complications of inflammation, albeit with the potential risk of neurotoxicity.

Accordingly, over a period of about 2 years, the child diagnosed with ALL receives aggressive treatments which, given at a time when major developmental changes are taking place, can disrupt brain development.[4] Treatments with or without irradiation are associated with long-term neurocognitive sequelae in survivors expressed by reduced scores on the

neuropsychological assessment of intellectual and executive functioning [5–8], as well as damage to brain tissue, mainly white matter (WM).[9–11] Several risk factors contribute to the development of neurocognitive complications: younger age at diagnosis, female sex, cranial radiotherapy (CRT), and overall treatment intensity.[12–15]

Part of the neurotoxicity of oncological treatments results in demyelination of the WM.[16] Particularly in children, newly synthesized myelin is even more vulnerable due to its higher metabolic activity and lower stability.[4] The emergence of late neurocognitive impairments is thought to be influenced by the level of premorbid brain integrity and the extent of neurotoxic effects, which involve direct WM impairments as well as disruption of mechanisms that facilitate tissue remyelination and compensatory processes.[17, 18] As a result, survivors of ALL often show neurocognitive impairments such as WM volume loss and disrupted WM integrity.[19] Various methods have been employed to capture WM abnormalities in long-term ALL survivors' brains. According to Wu et al. (2012), magnetization transfer ratio (MTR) is highly sensitive to myelin content and axonal density and can detect subtle brain abnormalities that are not apparent in conventional magnetic resonance imaging techniques. The extent to which the WM microstructural integrity at adult age determines the ensuing cognitive functioning of ALL survivors remains unclear.

According to the foregoing, the aim of this study is to investigate WM structural and microstructural integrity in long-term ALL survivors using volumetric investigation and magnetization transfer imaging. WM volumes and MTR are investigated, on the one hand, in relation to neuropsychological outcomes and, on the other hand, in relation to

neurocognitive risk factors (i.e., age at diagnosis, sex and adjunctive CRT), cumulative doses of corticosteroids (i.e., prednisone, hydrocortisone, and dexamethasone) and intrathecal chemotherapy agents (i.e., IT-cytarabine, IT-methotrexate, IT-hydrocortisone).

In addition to whole-brain measurements, a particular interest was carried toward the corpus callosum (CC). The CC is the largest WM fiber bundle connecting the two cerebral hemispheres. The integrity of the interhemispheric connection pathways is essential for the proper functioning of the brain. Several studies observed microstructural changes in the CC following oncological treatments based on systemic chemotherapy.[20–24] To date, very few studies have focused on the MTR. This study will enable a comprehensive examination of dose-related effects on magnetization transfer measures.

Drawing from the earlier context, our study's hypotheses are as follows. Firstly, we anticipate observing decreased white matter (WM) volume and magnetization transfer ratio (MTR) means among long-term ALL survivors in comparison to the healthy control group. Secondly, higher cumulative doses of chemotherapy agents are expected to correlate with worse neuroimaging measures and cognitive performance. Lastly, we hypothesize that MTR may specifically serve as an indicator of neurotoxic damage in ALL survivors, and this assertion will be examined through hierarchical multiple regression analyses.

Methods

Study Design and Recruitment

This retrospective study is part of the PETALE research program at Sainte-Justine University Health Center (SJUHC), Quebec, Canada, which was designed to identify and characterize ALL long-term complication biomarkers. As described in Marcoux et al. (2017), the PETALE cohort is composed of 246 ALLs diagnosed between age 0 and age 17, treated with the Dana Farber Cancer Institute protocols 87-01 to 05-01, and at least 5 years post-diagnosis at the data collection time point, without any history of refractory ALL, disease recurrence, or hematopoietic stem cell transplantation. According to their performance at the DIVERGT screening procedure[5, 26], a sample of 35 ALL survivors (age range [17 – 40]), aiming to represent all spectrum of cognitive performance found in the initial cohort, was selected, tested using anatomical MRI studies and included in this study. For comparison purposes, 21 age- and education level-matched healthy controls (age range [19 – 36]), representative with respect to sex, with no history of neurological, psychological or cancer disorders, were recruited within SJUHC Research Center and within social networks. The complete recruitment procedure is detailed elsewhere.[27] The study was approved by the Institutional Review Board of SJUHC, and investigations were carried out in accordance with the principles of the Declaration of Helsinki. Written informed consent was obtained from study participants or parents/guardians.

Study Procedures

Data collection

Neuroimaging protocol

MRI was performed on a General Electric Discovery MR750 3 Tesla system at SJUHC. MT spoiled gradient echo (MT-SPGR)[28] was used as acquisition method for magnetization transfer imaging by means of the following imaging sequences: 3D T_1-weighted inversion-recovery magnetization prepared–ultrafast acquisition gradient echo (IR-FSPGR) [repetition time (TR)/echo (TE): 8.16/3.18ms, inversion time (TI): 450ms, matrix: 256x256x188, field of view (FOV): 0.75x0.75x1.5mm and flip angle: 9°], 3D SPGR (MT saturation pulse off) and 3D MT-SPGR (MT saturation pulse on) [TR/TE: 32/4ms, matrix: 256x256x104, FOV: 0.75x0.75x1.5mm and flip angle: 10°].

Neuroimaging postprocessing

Images postprocessing was conducted using the FreeSurfer Software Suite [29] (http://surfer.nmr.mgh.harvard.edu/). Each participant's MRI data were processed independently to produce one mask per participant. This cortical reconstruction pipeline includes non-parametric non-uniform intensity normalization, automated Talairach transformation, skull-stripping[30], segmentation of the subcortical white matter[31], intensity normalization[32], tessellation, surface smoothing, inflation, quasi-homeomorphic spherical transformation, and automated topology correction[33]. As a result, 256 axial slices without gaps covering the entire brain were obtained from both 3D SPGR and 3D SPGR-MT, thereby acquiring an unsaturated data set and a saturated data set. Additionally, segmentation masks

were generated from the 3D T_1 IR-FSPGR evenly processed data set. The segmentation of WM volumes of interest (VOIs) implied automated and customized procedures. The segmentation of the whole brain subcortical WM and its right and left hemispheres' parcellation has been efficiently executed through FreeSurfer's automated process, although the CC segmentation required manual correction due to the undesired inclusion of neighbouring voxels, mostly from the fornix. CC was divided into five equal sections along length, enabling interhemispheric communication that supports distinct cognitive functions – anterior, mid-anterior, central, mid-posterior, and posterior sections correspond to rostrum, genu, body, isthmus, anterior splenium, and posterior splenium, respectively. Intracranial volume and cerebral WM volume in mm^3 were computed with FreeSurfer. Intracranial volume was estimated using an atlas normalization procedure.[34]

Magnetization transfer processing

To generate MTR data, each participant's MRI data were processed independently with an FSL pipeline (FMRIB Software). Images co-registration was performed using FLIRT[35] linear registration algorithm. Since SPGR data featured a higher defined contrast, it has been selected as reference images. Hence, MT-SPGR data was normalized to SPGR data to create a reference volume, which was then spatially co-registered to the whole head high-resolution T_1-weighted IR-FSPGR. To assure a proper comparison, an optimized registration procedure involving a rigid body transformation with 6 degrees of freedom was used. The resulting co-registered images were used to calculate the MTR maps voxel-by-voxel via the fslmaths program according to the following formula: MTR = (SPGR – (SPGR-MT))/SPGR. To extract MTR data from each VOIs,

a simple intersection between the 3D MTR data maps and the segmentation masks was possible since the MTR data volume and all MRI images of the same participant has been previously recalibrated and standardized. The corresponding voxels were intersected with the VOIs' coordinates in the segmentation masks. An outlier's correction fixed at ±1 standard deviation (SD) was then applied to our voxel-wise MTR data set to avoid potential errors affecting the MTR mean in CC VOIs due to imperfections in the CC segmentation and parcellation. Mean MTR was computed and defined as the average MTR of all voxels in each 3D VOIs: whole brain WM, left hemisphere WM, right hemisphere WM, whole CC, anterior CC, mid-anterior CC, mid-posterior CC, central CC, posterior CC.

Cognitive Assessment

All participants enrolled in the study were evaluated using a set of neuropsychological tests covering intellectual and executive functioning. The neuropsychological evaluation was conducted by a qualified examiner through a standardized testing protocol that is already detailed in Boulet-Craig et al. (2018). Intellectual functioning was assessed with the 10 core subtests of the Wechsler Adult Intelligence Scale 4th edition (WAIS-IV)[36]. Age-adjusted scores of the domain-specific WAIS-IV subtests were summarized and transformed into the four WAIS-IV indexes (i.e., Verbal Comprehension Index (VCI), Perceptual Reasoning Index (PRI), Working Memory Index (WMI) and Processing Speed Index (PSI)) along with the Full-Scale IQ (FSIQ) and the General Ability Index (GAI). These WAIS-IV index scores, in addition to the FSIQ and the GAI, are standardized to a mean of 100, with one standard deviation reflected in 15-point increments. Executive functioning was assessed with a DIVERGT[26] equivalent battery

including Digit Span[36], Verbal Fluency subtests[37], Trail Making Test[37] and Grooved Pegboard Test[38]. Raw scores were converted to age-adjusted scaled scores (mean [M] = 10, standard deviation [SD] = 3) based on nationally representative normative data. With the intention of quantifying the extent of ALL-associated cognitive sequelae on a singular composite score reflecting the most common executive deficits following ALL (i.e., working memory, verbal fluency, cognitive flexibility, and visuomotor processing speed), a global index of executive functioning was calculated for each participant. This Executive Functioning Index was obtained by computing the arithmetic mean of the following subtests' scaled scores: Digit Span, Verbal Fluency – Condition 1, Trail Making Test – Condition 4 and Grooved Pegboard – Dominant Hand.

Statistical Analysis

All analyses were carried out using IBM SPSS statistics 28. Initial group comparisons were conducted to ensure that ALL survivors and controls were matched on key demographic factors. Fischer's exact test was used to compare groups' sex ratios. An independent sample t-test and its nonparametric equivalent Mann-Whitney U test were respectively run to test for differences between groups in age at assessment and number of years of education.

Comparison of neuropsychological test results and neuroimaging outcomes between ALL survivors and controls were made using independent samples t-tests or Mann-Whitney U for non-normally distributed variables. Test results were examined for effect sizes using Pearson's correlation coefficient *r*. The magnitude of the observed effect was considered small when *r* varied around .10, medium when *r* varied around .30, and large if *r* reached .50.[39]

To examine the relationship between neuropsychological outcomes and cumulative dose of the chemotherapy agents, we employed directional Pearson correlations, shedding light on potential dose-response effects. Neuroimaging outcomes were also examined for associations with cognitive function using directional Pearson correlations, and their covariation with the cumulative doses of chemotherapy agents. Where applicable, both survivors and controls were included in correlational analyses.

To further explore the potential influence of the female sex as a risk factor, we conducted additional two-way ANOVAs to investigate sex-group interactions, specifically assessing their impact on cognitive and neuroimaging outcomes. ANOVAs' effect sizes were assessed using partial η^2 ($\eta^2_{partial}$), where .01, .06, and .014 correspond to small, medium, and large effect sizes.[40]

Finally, hierarchical multiple regression analyses were carried out to study the relative contribution of the cumulative dose of chemotherapy agents among the risk factors (i.e., female sex, early age at diagnosis, and adjunctive CRT) in predicting MTR metrics in the brain at adulthood. Regression models were adjusted for current age. Interactions between dose and sex and between dose and age at diagnosis were also explored. Effects sizes were interpreted using R^2 as a percentage of variance explained, where 1%, 9%, and 25% respectively indicated small, medium, and large effects.[40]

Given the well-documented neurocognitive sequelae in ALL survivors and our a priori hypothesis regarding their overall lower brain integrity compared to healthy controls, we conducted one-tailed tests. Test results were examined for statistical significance ($p \leq .05$). To

be aware of type 1 errors, the Benjamini-Hochberg false discovery rate (FDR) procedure[41, 42] was applied for multiple comparisons[43]. In correlational analyses, the FDR correction was applied on a dependent variable-by-dependent variable basis. Considering that the correction for multiplicity may increase the risk of type 2 errors[44], uncorrected *p*-values are reported throughout the manuscript, and FDR-adjusted *p*-values (FDR adj.-*p*) are also provided where appropriate. The FDR threshold was fixed at 0.05.

Results

Demographic variables and treatment characteristics are displayed in **Table 1**. ALL survivors were assessed in neuropsychology and neuroimaging for the present study on average at 18.90±5.37 years post-diagnosis and are therefore considered very long-term survivors. Neuropsychological outcomes are presented in **Table 2**. ALL survivors did not differ from controls either on the working memory index (WMI) (*p*=.623) or on the perceptual reasoning index (PRI) (*p*=.132). However, in comparison to the control group, ALL survivors exhibit lower average scores for the full-scale IQ (FSIQ) (*p*=.008, FDR adj.-*p*=.022), the general ability index (GAI) (*p*=.013, FDR adj.-*p*=.024), the verbal comprehension index (VCI) (*p*=.008, FDR adj.-*p*=.022) and the processing speed index (PSI) (*p*=.003, FDR adj.-*p*=.022). On the Executive Functioning Index based on DIVERGT scores, survivors underperformed compared to controls (*p*=.012, FDR adj.-*p*=.024), suggesting relative weakness in executive functioning. ALL survivors' scores were inferior to controls on the Trail making test condition 4 (*p*=.016, FDR adj.-*p*=.022) and on the Grooved pegboard (*p*=.005, FDR adj.-*p*=.022), which may reflect more specific executive weaknesses in cognitive flexibility and visuomotor processing speed. ALL survivors'

scores on the Digit span (p=.465) and on the Verbal fluency condition 1 (p=.248) did not differ from those of the controls.

Table 1. Demographics and clinical information

	ALL survivors (n = 35)	Controls (n = 21)	p
Demographics			
Sex, n (%)			
Male	21 (60)	12 (57.1)	1.00[c]
Female	14 (40)	9 (42.9)	
Age at assessment	26.27 (6.39)	27.1 (4.7)	.620[d]
Years of education	12.63 (2.18)	15.00 [11.00-18.00][b]	.080[e]
Treatment characteristics			
Age at diagnosis[a]	7.37 (5.55)	N/A	-
DFCI protocol, n (%)			
87-01	5 (14.3)	N/A	-
91-01	11 (31.4)	N/A	-
95-01	13 (37.1)	N/A	-
00-01	3 (8.6)	N/A	-
05-01	3 (8.6)	N/A	-
Cranial radiation therapy, n (%)			
Yes*	27 (71.1)	N/A	-
No	8 (22.9)	N/A	-
Chemotherapy cumulative doses			
IT methotrexate (mg/m^2)	134.35 (54.42)[a]	N/A	-
IT cytarabine (mg/m^2)	513.11 (197.65)[a]	N/A	-
IT hydrocortisone (mg/m^2)	22.39 [8.20 – 268.67][b]	N/A	-
IV methotrexate (mg/m^2)	6042.06 [1777.47 – 12750.46][b]	N/A	-
Effective corticosteroids dose (g/m^2)	12399.69 (5079.56)[a]	N/A	-

[a]Mean (Standard deviation); [b]Median [Range]; [c]Fisher's Exact Test; [d]Independent samples t-test; [e]Mann-Whitney U; DFCI: Dana-Farber Cancer Institute; *Median [range], 18 Gy [12-18 Gy]; IV: intravenous; IT: intrathecal

Table 2. Neuropsychological measures

	ALLs (*n* = 35)	Controls (*n* = 21)	*p*	FDR adj.-*p*	Effect size *r*
WAIS-IV scales					
FSIQ	94.14 (14.35)[a]	104.9 (13.7)[a]	**.008**[d]	**.022**	0.35
GAI	99.66 (11.81)[a]	108.5 (13.5)[a]	**.013**[d]	**.024**	0.33
VCI	98.23 (11.64)[a]	111 [83-123][b]	**.008**[e]	**.022**	0.35
PRI	101.20 (14.57)[a]	107.2 (13.8)[a]	.132[d]	.182	0.20
WMI	94.40 (13.54)[a]	94 [76-137][b]	.623[e]	.623	0.07
PSI	90.42 (20.63)[a]	104.4 (12.7)[a]	**.003**[d]	**.022**	0.39
DIVERGT scales					
Executive Functioning Index	8.70 (2.50)[a]	10.10 (1.50)[a]	**.012**[d]	**.024**	0.33
Digit span	7.00 [3.00-14.00][b]	8.86 (2.39)[a]	.465[e]	.512	0.10
Verbal fluency condition 1	7.91 (3.02)[a]	8.86 (2.74)[a]	.248[d]	.303	0.16
Trail making test condition 4	10.00 [1.00-15.00][b]	11.00 [8.00-14.00][b]	**.016**[e]	**.022**	0.31
Grooved pegboard dominant hand	8.74 (3.36)[a]	11.24 (2.59)[a]	**.005**[d]	**.022**	0.37

[a]Mean (Standard deviation); [b]Median **[**Range**]**; [c]Fisher's Exact Test; [d]Independent samples t-test; [e]Mann-Whitney U

Values in bold where $p \leq 0.05$ (2-tailed).

Table 3 presents the correlation analyses between the cumulative doses of chemotherapy agents received during treatments and the neuropsychological outcomes in adulthood. At first sight, IT-MTX stands out through the substantial correlations observed between its cumulative dose and several indices of cognitive performance (i.e., FSIQ, GAI, PRI, WMI, EF index), suggesting a higher dose of IT-MTX is associated with poorer general intellectual abilities, working memory and executive functioning. Nonetheless, the FDR correction led to the loss of statistical significance for the associations with the WMI and EF

index. Additionally, we found moderate to strong negative correlations between the total IT-cytarabine dose, and FSIQ, GAI and PRI. After considering the multiplicity correction, these results still demonstrated statistical significance. In contrast to the other IT agents, no significant correlations were observed between IT-hydrocortisone dosage and neuropsychological outcomes. Additionally, no evidence of associations was observed between the intravenous MTX dose or the effective corticosteroids dose, and the neuropsychological measures.

Table 3. Pearson's r for correlations conducted between cumulative doses of chemotherapy agents and neuropsychological indices

	FSIQ	GAI	VCI	PRI	WMI	PSI	EF index
IT-MTX dose	**-0.391*** **p=.010** **p_{adj}=.033**	**-0.387*** **p=.011** **p_{adj}=.027**	-0.104 p=.276 p_{adj}=.380	**-0.501**** **p=.001** **p_{adj}=.005**	**-0.295*** **p=.043** p_{adj}=.215	-0.250 p=.080 p_{adj}=.183	**-0.305*** **p=.037** p_{adj}=.125
IT-cytarabine dose	**-0.375*** **p=.013** **p_{adj}=.033**	**-0.397**** **p=.009** **p_{adj}=.027**	-0.131 p=.226 p_{adj}=.380	**-0.486**** **p=.002** **p_{adj}=.005**	-0.221 p=.101 p_{adj}=.253	-0.276 p=.060 p_{adj}=.183	-0.282 p=.050 p_{adj}=.125
IT-hydrocortisone dose	0.130 p=.479 p_{adj}=.479	-0.150 p=.476 p_{adj}=.476	-0.121 p=.311 p_{adj}=.380	-0.183 p=.226 p_{adj}=.377	-0.159 p=.258 p_{adj}=.323	0.134 p=.304 p_{adj}=.317	0.850 p=.365 p_{adj}=.426
IV-MTX dose	0.091 p=.302 p_{adj}=.378	0.027 p=.440 p_{adj}=.476	0.054 p=.380 p_{adj}=.380	-0.037 p=.417 p_{adj}=.417	0.153 p=.189 p_{adj}=.315	0.086 p=.317 p_{adj}=.317	0.033 p=.426 p_{adj}=.426
Effective corticosteroids dose	-0.156 p=.186 p_{adj}=.310	-0.132 p=.225 p_{adj}=.375	-0.153 p=.189 p_{adj}=.380	-0.066 p=.353 p_{adj}=.417	-0.025 p=.444 p_{adj}=.444	-0.219 p=.110 p_{adj}=.183	-0.169 p=.166 p_{adj}=.277

MTX: methotrexate; IT: intrathecal; IV: intravenous; p_{adj}: FDR adjusted p-values
* Correlation is significant at the 0.05 level (1-tailed).
** Correlation is significant at the 0.01 level (1-tailed).
Note: p-values adjusted for FDR separately for each dependent variable (neuropsychological indices).

Brain volumes outcomes are provided in **Table 4**. ALL survivors evidenced a 6.7% smaller WM volume (t(54)=-1.87, p=.034, FDR adj.-p=.057, r=.25) as well as a 5.3% smaller intracranial volume (t(54)=-1.81, p=.038, FDR adj.-p=.057, r=.24) than controls. Intracranial

volume is known as a proxy of the maximal brain volume attained following development. Therefore, comparisons were also made for WM volume fraction, which is the ratio between cerebral WM volume and intracranial volume. WM volume fraction was 1.4% smaller in ALL survivors compared to controls ($t(54)$=-0.78, p=.219, FDR adj.-p=.219, r=.11). Thereby, the WM volume difference wasn't statistically significant after adjusting for intracranial volume. Otherwise, the intracranial volume was not associated with age at the MRI time-point in ALL survivors and controls combinedly and neither was the WM volume. In an interesting way, there was a trend between younger age at diagnosis and smaller intracranial volume (r=.266, p=.061).

Table 4. Brain volume outcomes (mm^3)

	ALLs (n = 35) mean (SD)	**Controls (n = 21) mean (SD)**	***p***	**FDR adj.-*p***	**Effect size *r***
WM volume	412671.988 (55115,5779)	442292.971 (61429.4994)	**.034**	.057	0.25
Intracranial vol.	1 339179.48 (150168.331)	1413861.25 (149162.932)	**.038**	.057	0.24
WM vol. fraction	0.30795248 (0.02001171)	0.3122635 (0.01997215)	.219	.219	0.11

WM: White matter; vol.: volume
Values in bold where $p < 0.05$ (1-tailed).
Online only (supplemental material)

Table 5. Magnetization transfer imaging outcomes (MTR means)

	ALLs (n = 35)	**Controls (n = 21)**	***p***	**FDR adj.-*p***	**Effect size *r***
Whole brain	0.5760 (0.0120)[a]	0.5817 (0.0113)[a]	**.044**[c]	.097	0.23
Right hemisphere	0.5777 (0.0130)[a]	0.5837 (0.0112)[a]	**.044**[c]	.097	0.23
Left hemisphere	0.5745 (0.0116)[a]	0.5798 (0.0115)[a]	**.050**[c]	.097	0.22
Corpus Callosum (CC)	0.5935 (0.0119)[a]	0.5976 (0.0125)[a]	.117[c]	.176	0.16
Anterior CC	0.6024 (0.0134)[a]	0.6064 (0.0155)[a]	.154[c]	.182	0.14

Mid-anterior CC	0.5859 [0.5611 – 0.6110][b]	0.5911 (0.0143)[a]	.182[d]	.182	0.12
Central CC	0.5740 [0.5297 – 0.6048][b]	0.5766 (0.0218)[a]	.054[d]	.097	0.22
Mid-posterior CC	0.5799 (0.0168)[a]	0.5872 (0.0144)[a]	.051[c]	.097	0.22
Posterior CC	0.6040 (0.0105)[a]	0.6067 (0.0113)[a]	.182[c]	.182	0.12

[a]Mean (Standard deviation); [b]Median [Range]; [c]Independent samples t-test; [d]Mann-Whitney U
Values in bold where $p \leq 0.05$ (1-tailed).
Online only (supplemental material)

Table 5 presents the magnetization transfer imaging outcomes. ALL survivors tend to exhibit lower MTR means compared to controls. The group differences (ALL survivors<controls) reached the threshold of statistical significance in the whole brain (t(54)=-1.74, p=.044, FDR adj.-p=.097, r=.23), the right hemisphere (t(54)=-1.74, p=.044, FDR adj.-p=.097, r=.23) and the left hemisphere (t(54)=-1.67, p=.050, FDR adj.-p=.097, r=.22), yet the multiplicity correction rendered the findings statistically inconclusive. In addition, interestingly, differences in MTR means (ALL survivors<controls) were on the borderline of statistical significance for two sections of the CC, the central section (U=272, z=-1.62, p=.054, FDR adj.-p=.097, r=-.22) and the mid-posterior section (t(54)=-1.67, p=.051, FDR adj.-p=.097, r=.22). The central and mid-posterior sections of the CC cover the body, the isthmus, and the anterior splenium, carrying fibres connecting motor and premotor cortex, sensory cortex, association cortex and visual areas.[45, 46] These interhemispheric connections support motor planning, initiation and coordination, multimodal sensory processing, visual integration, and higher-order cognitive functions such as memory, language and problem-solving.[47–51] Microstructural damage in these regions of the CC could possibly contribute to the cognitive weaknesses observed in ALL survivors, especially visuomotor coordination and processing

speed. Nevertheless, our study did not yield a statistically significant difference in callosal regions' mean MTR, potentially attributable to limited statistical power.

Regarding the female sex risk factor, separate two-way ANOVAs were conducted to test for sex-group interactions, with neuropsychological and neuroimaging outcomes as dependent variables. No sex-group interaction was found to be significant. No main effect of sex was found on the neuropsychological outcomes. However, we observed a main effect of sex (females<males) on the WM volume (uncorrected for intracranial volume) ($F=21.23$, $\eta^2_{partial}=.290$, $p<.001$, FDR adj.-$p=.001$), the intracranial volume ($F=20.51$, $\eta^2_{partial}=.283$, $p<.001$, FDR adj.-$p=.001$), and the CC mean MTR ($F=8.23$, $\eta^2_{partial}=.136$, $p=.006$, FDR adj.-$p=.018$). Otherwise, no main effect of sex was found on the whole brain mean MTR ($p=.290$, FDR adj.-$p=.290$) nor on the WM volume fraction ($p=.075$, FDR adj.-$p=.092$). Indeed, men generally have larger head sizes and tend to exhibit larger brain volume in comparison to women.[52–54] Thus, sex differences in WM volume tend to disappear when considering intracranial volume. Further, an effect of sex on the MTR of the corpus callosum has been reported in normal adults; however, the literature remains inconsistent, with some studies suggesting that males exhibit higher callosal MTR values than females. For example, Björnholm and colleagues (2017) found sex-related differences in all sections of the CC among 433 all-comer adults (mean age=26.50, SD=0.51). However, other studies have found none.[56, 57]

Correlation analyses between neuroimaging outcomes and neuropsychological measures are presented in **Table 6**. Without adjustment for intracranial volume, the MW volume was correlated to FSIQ ($r=.227$,$p=.046$, FDR adj.-$p=.108$), GAI ($r=.368$, $p=.003$, FDR adj.-$p=.009$), VCI ($r=.355$, $p=.004$, FDR adj.-$p=.012$) and PRI ($r=.246$, $p=.034$, FDR adj.-$p=.075$). After

the FDR correction for multiple comparisons, only the associations with GAI and VCI remained significant. The WM volume fraction was correlated to GAI (r=239, p=.038, FDR adj.-p=.038) and VCI (r=.232, p=.043, FDR adj.-p=.043), and the findings were unaffected by the FDR correction.

Moreover, the whole brain mean MTR was associated with GAI (r=.227, p=.046, FDR adj.-p=.067) and VCI (r=.239, p=.038, FDR adj.-p=.057). The right hemisphere MTR mean was associated to FSIQ (r=.234, p=.041, FDR adj.-p=.115), GAI (r=.241, p=.037, FDR adj.-p=.067), VCI (r=.240, p=.037, FDR adj.-p=.057) and PSI (r=.260, p=.029, FDR adj.-p=.125). The left hemisphere MTR mean was associated with VCI (r=.228, p=.046, FDR adj.-p=.059). The mean MTR in the CC was correlated with GAI (r=.259, p=.027, FDR adj.-p=.067) and VCI (r=.271, p=.022, FDR adj.-p=.057). Several statistically significant correlations were also found for different callosal sections. The mean MTR in the anterior section correlated with GAI (r=.228, p=.045, FDR adj.-p=.451). The mean MTR in the mid-anterior section correlated with FSIQ (r=.244, p=.035, FDR adj.-p=.115), GAI (r=.282, p=.018, FDR adj.-p=.067), VCI (r=.243, p=.035, FDR adj.-p=.057) and PRI (r=.249, p=.032, FDR adj.-p=.239). The mean MTR in the mid-posterior section correlated with FSIQ (r=.232, p=.043, FDR adj.-p=.115), GAI (r=.238, p=.039, FDR adj.-p=.067) and VCI (r=.278, p=.019, FDR adj.-p=.057). The mean MTR in the posterior section correlated with VCI (r=.258, p=.027, FDR adj.-p=.057). On the other hand, all these associations with MTR means were no longer significant after the multiplicity correction.

Table 6. Pearson's r for directional correlations conducted between neuroimaging outcomes and neuropsychological indices

	FSIQ	GAI	VCI	PRI	WMI	PSI	EF index
MTR means							
Whole brain	0.203 *p*=.067 p_{adj}=.115	**0.227*** ***p*=.046** p_{adj}=.067	**0.239*** ***p*=.038** p_{adj}=.057	0.141 *p*=.151 p_{adj}=.239	0.023 *p*=.432 p_{adj}=.498	0.200 *p*=.073 p_{adj}=.125	0.081 *p*=.277 p_{adj}=.409
Right hemisphere	**0.234*** ***p*=.041** p_{adj}=.115	**0.241*** ***p*=.037** p_{adj}=.067	**0.240*** ***p*=.037** p_{adj}=.057	0.160 *p*=.120 p_{adj}=.239	0.051 *p*=.355 p_{adj}=.498	**0.260*** ***p*=.029** p_{adj}=.125	0.131 *p*=.168 p_{adj}=.409
Left hemisphere	0.159 *p*=.121 p_{adj}=.156	0.201 *p*=.069 p_{adj}=.078	**0.228*** ***p*=.046** p_{adj}=.059	0.109 *p*=.212 p_{adj}=.239	-0.007 *p*=.480 p_{adj}=.498	0.130 *p*=.174 p_{adj}=.224	0.022 *p*=.437 p_{adj}=.437
Corpus callosum (CC)	0.215 *p*=.056 p_{adj}=.115	**0.259*** ***p*=.027** p_{adj}=.067	**0.271*** ***p*=.022** p_{adj}=.057	0.170 *p*=.105 p_{adj}=.239	0.052 *p*=.351 p_{adj}=.498	0.192 *p*=.083 p_{adj}=.125	0.065 *p*=.318 p_{adj}=.409
Anterior CC	0.193 *p*=.077 p_{adj}=.115	**0.228*** ***p*=.045** p_{adj}=.451	0.212 *p*=.058 p_{adj}=.065	0.174 *p*=.100 p_{adj}=.239	0.022 *p*=.436 p_{adj}=.498	0.193 *p*=.081 p_{adj}=.125	0.091 *p*=.253 p_{adj}=.409
Mid-anterior CC	**0.244*** ***p*=.035** p_{adj}=.115	**0.282*** ***p*=.018** p_{adj}=.067	**0.243*** ***p*=.035** p_{adj}=.057	**0.249*** ***p*=.032** p_{adj}=.239	0.094 *p*=.246 p_{adj}=.498	0.214 *p*=.060 p_{adj}=.125	0.128 *p*=.174 p_{adj}=.409
Central CC	-0.022 *p*=.435 p_{adj}=.435	-0.017 *p*=.451 p_{adj}=.451	0.011 *p*=.468 p_{adj}=.468	-0.026 *p*=.426 p_{adj}=.426	-0.046 *p*=.370 p_{adj}=.498	0.005 *p*=.486 p_{adj}=.486	-0.073 *p*=.298 p_{adj}=.409
Mid-posterior CC	**0.232*** ***p*=.043** p_{adj}=.115	**0.238*** ***p*=.039** p_{adj}=.067	**0.278*** ***p*=.019** p_{adj}=.057	0.123 *p*=.184 p_{adj}=.239	0.095 *p*=.244 p_{adj}=.498	0.194 *p*=.080 p_{adj}=.125	0.107 *p*=.215 p_{adj}=.409
Posterior CC	0.147 *p*=.139 p_{adj}=.156	0.219 *p*=.052 p_{adj}=.067	**0.258*** ***p*=.027** p_{adj}=.057	0.111 *p*=.208 p_{adj}=.239	0.001 *p*=.498 p_{adj}=.498	0.115 *p*=.204 p_{adj}=.229	-0.044 *p*=.373 p_{adj}=.420
Volumes							
White matter (WM)	**0.227*** ***p*=.046** p_{adj}=.108	**0.368**** ***p*=.003** **p_{adj}=.009**	**0.355**** ***p*=.004** **p_{adj}=.012**	**0.246*** ***p*=.034** p_{adj}=.075	0.021 *p*=.439 p_{adj}=.439	0.067 *p*=.314 p_{adj}=.371	0.149 p=.137 p_{adj}=.199
Intracranial volume	0.192 *p*=.078 p_{adj}=.108	**0.324**** ***p*=.007** **p_{adj}=.011**	**0.311**** ***p*=.010** **p_{adj}=.015**	**0.222*** ***p*=.050** p_{adj}=.075	-0.063 *p*=.321 p_{adj}=.439	0.074 *p*=.297 p_{adj}=.371	0.115 *p*=.199 p_{adj}=.199
WM volume fraction	0.168 *p*=.108 p_{adj}=.108	**0.239*** ***p*=.038** **p_{adj}=.038**	**0.232*** ***p*=.043** **p_{adj}=.043**	0.151 *p*=.133 p_{adj}=.133	0.152 *p*=.131 p_{adj}=.393	0.046 *p*=.371 p_{adj}=.371	0.130 *p*=.169 p_{adj}=.199

p_{adj}: FDR adjusted *p*-values

* Correlation is significant at the 0.05 level (1-tailed).** Correlation is significant at the 0.01 level (1-tailed).

Note: *p*-values adjusted for FDR separately for each dependent variable (neuropsychological indices) for MTRs and volumes separately
Online only (supplemental material)

Correlation analyses between neuroimaging outcomes and chemotherapy agents' cumulative doses are presented in **Table 7**. No association between WM volume and cumulative doses was found. The effective corticosteroid cumulative dose was associated with smaller intracranial volume in survivors (*r*=-.298, *p*=.041, FDR adj.-*p*=.068), yet the multiplicity correction rendered those findings statistically inconclusive. No association was found between intravenously administered MTX dosage and the neuroimaging outcomes, suggesting less neurotoxicity from intravenous administration compared to IT administration. In agreement with the above, cumulative doses of intrathecally administered chemotherapy, including MTX, demonstrated substantial negative correlations with the MTR means. Higher IT-MTX dose was associated with a smaller mean MTR in the whole brain (*r*=-.403, *p*=.008, FDR adj.-*p*=.015), the right hemisphere (*r*=-.434, *p*=.005, FDR adj.-*p*=.013), the left hemisphere (*r*=-.347, *p*=.021, FDR adj.-*p*=.035), the whole CC (*r*=-.283, *p*=.050, FDR adj.-*p*=.083) and its anterior section (*r*=-.351, *p*=.019, FDR adj.-*p*=.048). The correlations between IT-MTX dosages and MTR means maintained their statistical significance after the FDR correction except for the whole CC. Similar results have been found for IT-cytarabine. The IT-cytarabine cumulative dose was negatively correlated with the mean MTR in the whole brain (*r*=-.405, *p*=.008, FDR adj.-*p*=.015), the right hemisphere (*r*=-.437, *p*=.004, FDR adj.-*p*=.013), the left hemisphere (*r*=-.349, *p*=.020, FDR adj.-*p*=.035), the whole CC (*r*=-.284, *p*=.049, FDR adj.-*p*=.083) and its anterior section (*r*=-.359, *p*=.017, FDR adj.-*p*=.048). These associations survived correction for multiple

comparisons except for the whole CC. As IT-MTX and IT-cytarabine dosages were strongly related to each other in our sample (r=.954, p<001), it is unclear whether neurotoxic effects arise more from one IT agent or the other or from both. Nevertheless, the long-term neurotoxicity of MTX is widely documented in the literature.[58–61] MTX is identified among the most neurotoxic chemotherapy agents while the possibility of a harmful interaction between IT-MTX and IT-cytarabine has been recently raised.[62] Furthermore, the IT-hydrocortisone cumulative dose was negatively correlated with the mean MTR in the whole brain (r=-.533, p=.009, FDR adj.-p=.015), the right hemisphere (r=-.532, p=.009, FDR adj.-p=.015), the left hemisphere (r=-.512, p=.013, FDR adj.-p=.035), the whole CC (r=-.398, p=.046, FDR adj.-p=.083), and its anterior section (r=-.405, p=.043, FDR adj.-p=.072), mid-anterior section (r=-.465, p=.022, FDR adj.-p=.110) and mid-posterior section (r=-.393, p=.048, FDR adj.-p=.240). After FDR correction, the dosage associations with the mean MTR in the whole brain, the right hemisphere, and the left hemisphere maintained their statistical significance. Note that the IT-hydrocortisone dosages were not correlated with the IT-MTX (p=.286) and IT-cytarabine dosages (p=.320). **Figure 1** displays the scatter diagrams of the relationship between IT agents' dosage and the MTR mean in the whole brain.

Table 7. Pearson's r for directional correlations conducted between neuroimaging outcomes and cumulative doses of chemotherapy agents

	Effective corticosteroids	IV MTX	IT MTX	IT cytarabine	IT hydrocortisone
MTR means					
Whole brain	0.090 *p*=.303 p_{adj}=.379	0.020 *p*=.445 p_{adj}=.445	**-0.403**** ***p*=.008** **p_{adj}=.015**	**-0.405**** ***p*=.008** **p_{adj}=.015**	**-0.533**** ***p*=.009** **p_{adj}=.015**
Right hemisphere	0.079 *p*=.326 p_{adj}=.408	-0.034 *p*=.422 p_{adj}=.422	**-0.434**** ***p*=.005** **p_{adj}=.013**	**-0.437**** ***p*=.004** **p_{adj}=.013**	**-0.532**** ***p*=.009** **p_{adj}=.015**
Left hemisphere	0.097 *p*=.290 p_{adj}=.301	0.091 *p*=.301 p_{adj}=.301	**-0.347*** ***p*=.021** **p_{adj}=.035**	**-0.349*** ***p*=.020** **p_{adj}=.035**	**-0.512*** ***p*=.013** **p_{adj}=.035**
Corpus callosum (CC)	0.009 *p*=.480 p_{adj}=.480	0.111 *p*=.263 p_{adj}=.329	**-0.283*** ***p*=.050** p_{adj}=.083	**-0.284*** ***p*=.049** p_{adj}=.083	**-0.398*** ***p*=.046** p_{adj}=.083
Anterior CC	-0.045 *p*=.399 p_{adj}=.399	0.059 *p*=.369 p_{adj}=.399	**-0.351*** ***p*=.019** **p_{adj}=.048**	**-0.359*** ***p*=.017** **p_{adj}=.048**	**-0.405*** ***p*=.043** p_{adj}=.072
Mid-anterior CC	0.084 *p*=.316 p_{adj}=.395	-0.011 *p*=.476 p_{adj}=.476	-0.241 *p*=.081 p_{adj}=.135	-0.241 *p*=.081 p_{adj}=.135	**-0.465*** ***p*=.022** p_{adj}=.110
Central CC	0.052 *p*=.384 p_{adj}=.499	0.256 *p*=.069 p_{adj}=.345	-0.019 *p*=.457 p_{adj}=.499	0.000 *p*=.499 p_{adj}=.499	-0.104 *p*=.336 p_{adj}=.499
Mid-posterior CC	-0.021 *p*=.453 p_{adj}=.453	0.196 *p*=.130 p_{adj}=.248	-0.148 *p*=.198 p_{adj}=.248	-0.148 *p*=.198 p_{adj}=.248	**-0.393*** ***p*=.048** p_{adj}=.240
Posterior CC	0.070 *p*=.345 p_{adj}=.411	0.039 *p*=.411 p_{adj}=.411	-0.260 *p*=.066 p_{adj}=.123	-0.250 *p*=.074 p_{adj}=.123	-0.365 *p*=.062 p_{adj}=.123
Volumes					
White matter (WM)	-0.178 *p*=.153 p_{adj}=.255	0.381 *p*=.012 p_{adj}=.060	-0.097 *p*=.290 p_{adj}=.290	-0.103 *p*=.278 p_{adj}=.290	0.227 *p*=.125 p_{adj}=.255
Intracranial volume	**-0.298*** ***p*=.041** p_{adj}=.068	0.358 *p*=.017 p_{adj}=.068	-0.135 *p*=.219 p_{adj}=.219	-0.142 *p*=.208 p_{adj}=.219	0.413 *p*=.039 p_{adj}=.068
WM volume fraction	0.169 *p*=.166 p_{adj}=.345	0.157 *p*=.184 p_{adj}=.345	0.014 *p*=.469 p_{adj}=.495	-0.002 *p*=.495 p_{adj}=.495	-0.199 *p*=.207 p_{adj}=.345

CC: corpus callosum; WM: white matter; IV: intravenous; IT: intrathecal; p_{adj}: FDR adjusted *p*-values

* Correlation is significant at the 0.05 level (1-tailed).

** Correlation is significant at the 0.01 level (1-tailed).

Note: *p*-values adjusted for FDR separately for each dependent variable (volumes and MTR means).

Figure 1. Effect of cumulative dosage of intrathecal chemotherapy agents on the whole brain mean MTR: linear regression analysis

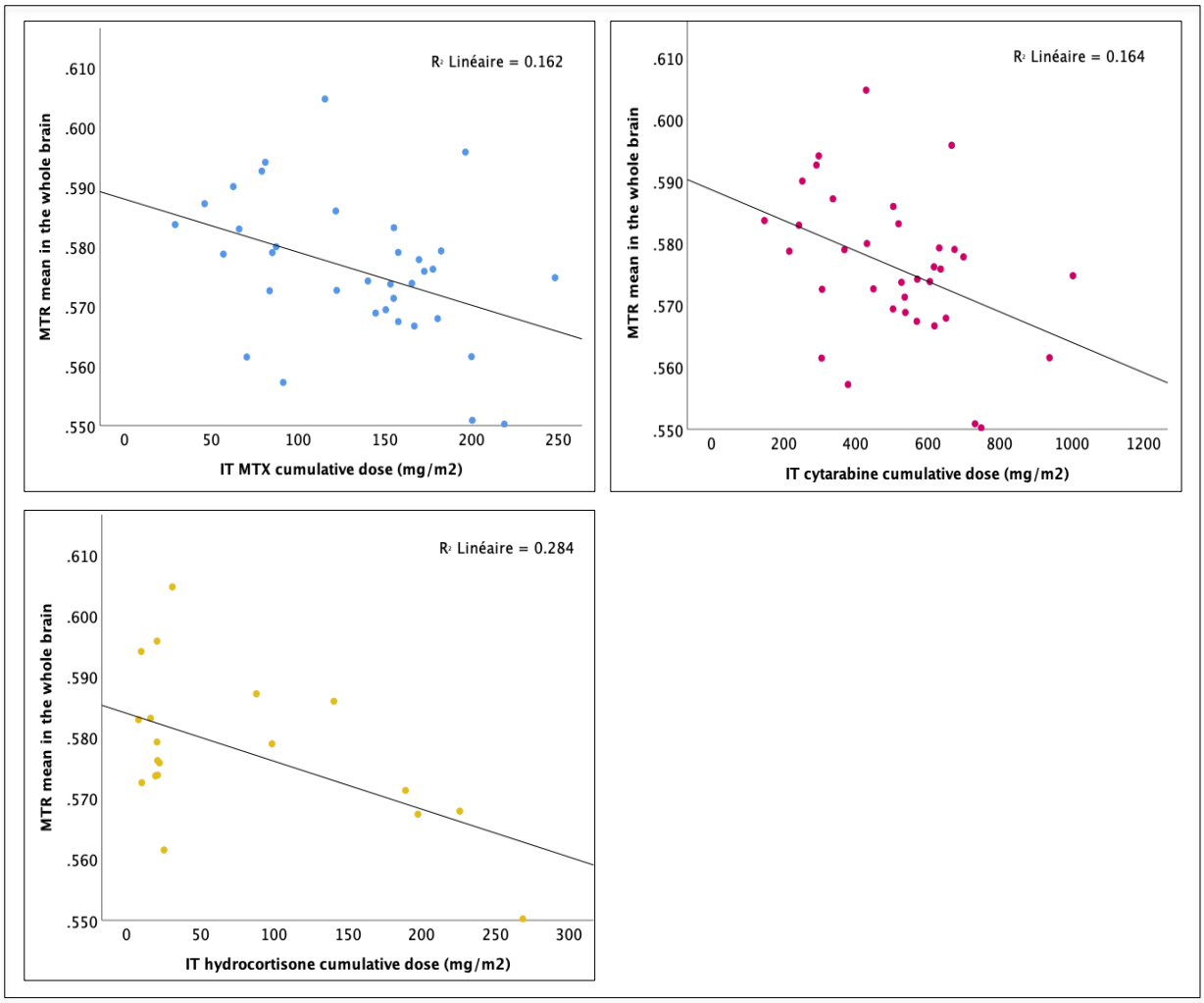

Based on the previous results, each of the IT agents (i.e., IT-MTX, IT-cytarabine, IT-hydrocortisone) was included as an independent variable separately in the multiple regression models with the mean MTR in the whole brain and the mean MTR in the CC as the dependent variables (6 regression models). In the first step of the regression models, current age (continuous variable), age at diagnosis (continuous variable), sex (binary variable), and adjunctive CRT (binary variable) were introduced using an enter method. In the second step, the cumulative dose of the chemotherapeutic agent (i.e., IT-MTX, IT-cytarabine, IT-hydrocortisone) was introduced. In the models including IT-MTX as a predictor, in the context of a sensitivity analysis, the cumulative leucovorin dose was introduced in the next step because of its potential neuroprotective effect suggested by previous studies.[14, 60] The purpose of this sensitivity analysis was to determine whether significant associations would be affected by the inclusion of the leucovorin dose as an additional factor. In the last step of all models, interactions between the dose of chemotherapy agents and sex, as well as the age at diagnosis were explored by adding interaction terms. The sex variable was coded with a value of 1 for female sex and 0 for male sex. The radiotherapy variable was coded with a value of 1 for treatment including CRT and 0 for chemotherapy-only treatment. All continuous predictors included in the regression models were centered around their mean, resulting in a transformation that set their means to 0. Interaction terms were calculated from the mean-centered predictors. Thus, beta coefficients should be interpreted as the average change in the outcome variable for a one-unit change in the predictor from its mean value. Standardized beta coefficients indicate the change in the outcome variable associated with a one-standard-

deviation change in the predictor, allowing for comparisons of the relative importance or strength of the predictors in influencing the outcome variable.

The regression models and associated statistics are presented in **Tables 8 to 13**. In the first step of the models, controlling for current age, the combination of the risk factors (i.e., age at diagnosis, sex, and CRT), explained, in a non-significant way, 18% of the variance of the mean MTR in the whole brain ($F_{4,30}$=1.623, *p*=.194), and in a significant way, 29% of the variance of the mean MTR in the CC ($F_{4,30}$=2.987, *p*=.035). No covariates were significant in the models predicting the mean MTR in the whole brain. Sex was found to be a significant covariate of the mean MTR in the CC (B=-.009, β=-.366, *p*=.039), with female sex associated with a reduced callosal mean MTR. In the following step, separately, the cumulative dose of IT-MTX, IT-cytarabine and IT-hydrocortisone respectively added a significant contribution of 16% ($\Delta F_{1,29}$=7.244, *p*=.012, β=-.704), 15% ($\Delta F_{1,29}$=6.353, *p*=.017, β=-.582), and 14% ($\Delta F_{1,29}$=5.917, *p*=.021, β=-.696) to the prediction of the mean MTR in the whole brain, and 11% ($\Delta F_{1,29}$=5.228, *p*=.030, β=-.574), 10% ($\Delta F_{1,29}$=4.536, *p*=.042, β=-.471), and 11% ($\Delta F_{1,29}$=5.016, *p*=.033, β=-.606) for the mean MTR in the CC. The inclusion of leucovorin did not impact the association between IT-MTX dose and the mean MTR in the whole brain or the CC. No dose interactions were found with sex or age at diagnosis.

Table 8. The relationship between age at diagnosis, sex, CRT, IT-MTX cumulative dose and whole brain mean MTR

	B	β	R	R^2	ΔR^2	F	ΔF	t
Step 1			.422	.178	.178	1.623 (*p*=.194)	1.623 (*p*=.194)	
Current age	.000	-.187						-.806 (*p*=.427)
Age at diagnosis	.001	.329						1.561 (*p*=.129)
Sex	-.003	-.129						-.710 (*p*=.483)
Cranial radiotherapy	.008	.281						1.634 (*p*=.113)
Step 2			.585	.342	.164	**3.018 (*p*=.026)**	**7.244 (*p*=.012)**	
Current age	-.001	-.316						-1.463 (*p*=.154)
Age at diagnosis	.000	-.136						-.526 (*p*=.603)
Sex	-.005	-.200						-1.192 (*p*=.243)
Cranial radiotherapy	.007	.253						1.619 (*p*=.116)
IT-MTX dose	.000	-.704						**-2.692 (*p*=.012)**
Step 3			.585	.342	.000	2.428 (*p*=.051)	.001 (*p*=.974)	
Current age	-.001	-.316						-1.435 (*p*=.162)
Age at diagnosis	.000	-.135						-.508 (*p*=.615)
Sex	-.005	-.202						-1.094 (*p*=.283)
Cranial radiotherapy	.007	.254						1.584 (*p*=.124)
IT-MTX dose	.000	-.702						**-2.586 (*p*=.015)**
Leucovorin dose	.000	-.006						-.033 (p=.974)
Step 4			.585	.343	.000	1.694 (*p*=.147)	.008 (*p*=.992)	
Current age	-.001	-.306						-1.103 (*p*=.280)
Age at diagnosis	.000	-.111						-.295 (*p*=.770)
Sex	-.005	-.203						-1.059 (*p*=.299)
Cranial radiotherapy	.007	.261						1.337 (*p*=.193)

IT-MTX dose	.000	-.692						-2.001 (*p*=.056)
Leucovorin dose	.000	-.010						-.051 (*p*=.959)
IT-MTX dose * sex	.000	.011						.041 (*p*=.968)
IT-MTX dose * age at diagnosis	.000	.026						.101 (*p*=.921)

B: beta; β: standardized beta; Δ: variation

Table 9. The relationship between age at diagnosis, sex, CRT, IT-MTX cumulative dose and corpus callosum mean MTR

	B	β	R	R^2	ΔR^2	F	ΔF	t
Step 1			.534	.285	.285	**2.987 (*p*=.035)**	**2.987 (*p*=.035)**	
Current age	.000	-.093						-.432 (*p*=.669)
Age at diagnosis	.000	.216						1.099 (*p*=.281)
Sex	-.009	-.366						**-2.160 (*p*=.039)**
Cranial radiotherapy	.009	.326						2.036 (*p*=.051)
Step 2			.628	.394	.109	**3.772 (*p*=.009)**	**5.228 (*p*=.030)**	
Current age	.000	-.199						-.959 (*p*=.345)
Age at diagnosis	.000	-.163						-.658 (*p*=.516)
Sex	-.010	-.424						**-2.636 (*p*=.013)**
Cranial radiotherapy	.008	.304						2.024 (*p*=.052)
IT-MTX dose	.000	-.574						**-2.286 (*p*=.030)**
Step 3			.628	.394	.000	**3.040 (*p*=.020)**	.018 (*p*=.895)	
Current age	.000	-.198						-.936 (*p*=.357)
Age at diagnosis	.000	-.159						-.623 (*p*=.538)
Sex	-.010	-.433						**-2.444 (*p*=.021)**
Cranial radiotherapy	.009	.306						1.991 (*p*=.056)
IT-MTX dose	.000	-.567						**-2.176 (*p*=.038)**
Leucovorin dose	.000	-.022						-.133 (p=.895)

Step 4			.641	.411	.017	2.268 (*p*=.055)	.366 (*p*=.697)	
Current age	.000	-.087						-.332 (*p*=.743)
Age at diagnosis	-.001	-.305						-.859 (*p*=.398)
Sex	-.010	-.434						**-2.390 (*p*=.024)**
Cranial radiotherapy	.007	.235						1.270 (*p*=.215)
IT-MTX dose	.000	-.718						**-2.196 (*p*=.037)**
Leucovorin dose	.000	.029						.159 (*p*=.875)
IT-MTX dose * sex	.000	.204						.796 (*p*=.433)
IT-MTX dose * age at diagnosis	.000	-.137						-.554 (*p*=.585)

B: beta; β: standardized beta; Δ: variation
Online only (supplemental material)

Table 10. The relationship between age at diagnosis, sex, CRT, IT-cytarabine cumulative dose and whole brain mean MTR

	B	**β**	**R**	**R^2**	**ΔR^2**	**F**	**ΔF**	**t**
Step 1			.422	.178	.178	1.623 (*p*=.194)	1.623 (*p*=.194)	
Current age	.000	-.187						-.806 (*p*=.427)
Age at diagnosis	.001	.329						1.561 (*p*=.129)
Sex	-.003	-.129						-.710 (*p*=.483)
Cranial radiotherapy	.008	.281						1.634 (*p*=.113)
Step 2			.571	.326	.148	**2.801 (*p*=.035)**	**6.353 (*p*=.017)**	
Current age	-.001	-.284						-1.311 (*p*=.200)
Age at diagnosis	.000	-.026						-.108 (*p*=.915)
Sex	-.005	-.186						-1.102 (*p*=.279)
Cranial radiotherapy	.008	.268						1.693 (*p*=.101)
IT-cytarabine dose	.000	-.582						**-2.521 (*p*=.017)**
Step 3			.573	.328	.002	1.882 (*p*=.112)	.046 (*p*=.956)	

Current age	-.001	-.278						-1.061 (*p*=.298)
Age at diagnosis	.000	-.096						-.278 (*p*=.783)
Sex	-.005	-.194						-1.094 (*p*=.284)
Cranial radiotherapy	.007	.243						1.326 (*p*=.196)
IT-cytarabine dose	.000	-.652						-1.950 (*p*=.062)
IT-cytarabine dose * sex	.000	.054						.209 (*p*=.836)
IT-cytarabine dose * age at diagnosis	.000	-.075						-.272 (*p*=.788)

B: beta; β: standardized beta; Δ: variation
Online only (supplemental material)

Table 11. The relationship between age at diagnosis, sex, CRT, IT-cytarabine cumulative dose and corpus callosum mean MTR

	B	**β**	**R**	**R^2**	**ΔR^2**	**F**	**ΔF**	**t**
Step 1			.534	.285	.285	**2.987 (*p*=.035)**	**2.987 (*p*=.035)**	
Current age	.000	-.093						-.432 (*p*=.669)
Age at diagnosis	.000	.216						1.099 (*p*=.281)
Sex	-.009	-.366						**-2.160 (*p*=.039)**
Cranial radiotherapy	.009	.326						2.036 (*p*=.051)
Step 2			.618	.382	.097	**3.579 (*p*=.012)**	**4.536 (*p*=.042)**	
Current age	.000	-.172						-.830 (*p*=.414)
Age at diagnosis	.000	-.071						-.310 (*p*=.759)
Sex	-.010	-.413						**-2.549 (*p*=.016)**
Cranial radiotherapy	.009	.316						**2.085 (*p*=.046)**
IT-cytarabine dose	.000	-.471						**-2.130 (*p*=.042)**
Step 3			.623	.389	.007	**2.451 (*p*=.044)**	.153 (*p*=.859)	
Current age	.000	-.118						-.472 (*p*=.641)
Age at diagnosis	.000	-.143						-.432 (*p*=.669)

Sex	-.010	-.428						**-2.528 (*p*=.018)**
Cranial radiotherapy	.008	.290						1.654 (*p*=.110)
IT-cytarabine dose	.000	-.576						-1.806 (*p*=.082)
IT-cytarabine dose * sex	.000	.137						.551 (*p*=.586)
IT-cytarabine dose * age at diagnosis	.000	-.058						-.220 (*p*=.828)

B: beta; β: standardized beta; Δ: variation
Online only (supplemental material)

Table 12. The relationship between age at diagnosis, sex, CRT, IT-cytarabine cumulative dose and corpus callosum mean MTR

	B	**β**	**R**	**R^2**	**ΔR^2**	**F**	**ΔF**	**t**
Step 1			.422	.178	.178	1.623 (*p*=.194)	1.623 (*p*=.194)	
Current age	.000	-.187						-.806 (*p*=.427)
Age at diagnosis	.001	.329						1.561 (*p*=.129)
Sex	-.003	-.129						-.710 (*p*=.483)
Cranial radiotherapy	.008	.281						1.634 (*p*=.113)
Step 2			.563	.317	.139	**2.695 (*p*=.041)**	**5.917 (*p*=.021)**	
Current age	-.001	-.557						**-2.118 (*p*=.043)**
Age at diagnosis	.001	.624						**2.712 (*p*=.011)**
Sex	-.006	-.261						-1.473 (*p*=.152)
Cranial radiotherapy	-.004	-.129						-.556 (*p*=.582)
IT-hydrocortisone dose	.000	-.696						**-2.433 (*p*=.021)**
Step 3			.565	.320	.002	1.812 (*p*=.126)	.046 (*p*=.955)	
Current age	-.001	-.626						-1.593 (*p*=.123)
Age at diagnosis	.001	.650						**2.564 (*p*=.016)**
Sex	-.008	-.329						-.505 (*p*=.618)
Cranial radiotherapy	-.004	.134						-.435 (*p*=.667)

IT-hydrocortisone dose	.000	-.750						**-2.062 (*p*=.049)**
IT-hydrocortisone dose * sex	.000	-.071						-.091 (*p*=.928)
IT-hydrocortisone dose * age at diagnosis	.000	-.060						-.295 (*p*=.770)

B: beta; β: standardized beta; Δ: variation
Online only (supplemental material)

Table 13. The relationship between age at diagnosis, sex, CRT, IT-hydrocortisone cumulative dose and corpus callosum mean MTR

	B	β	R	R^2	ΔR^2	F	ΔF	t
Step 1			.534	.285	.285	**2.987 (*p*=.035)**	**2.987 (*p*=.035)**	
Current age	.000	-.093						-.432 (*p*=.669)
Age at diagnosis	.000	.216						1.099 (*p*=.281)
Sex	-.009	-.366						**-2.160 (*p*=.039)**
Cranial radiotherapy	.009	.326						2.036 (*p*=.051)
Step 2			.625	.390	.105	**3.713 (*p*=.010)**	**5.016 (*p*=.033)**	
Current age	-.001	-.416						-1.672 (*p*=.105)
Age at diagnosis	.001	.472						**2.174 (*p*=.038)**
Sex	-.011	-.481						**-2.874 (*p*=.008)**
Cranial radiotherapy	-.001	-.030						-.137 (*p*=.892)
IT-hydrocortisone dose	.000	-.606						**-2.240 (*p*=.033)**
Step 3			.635	.403	.013	**2.605 (*p*=.034)**	.291 (*p*=.750)	
Current age	-.001	-.447						-1.215 (*p*=.235)
Age at diagnosis	.001	.435						1.830 (*p*=.078)
Sex	-.018	-.774						-1.269 (*p*=.215)
Cranial radiotherapy	.003	.096						.333 (*p*=.742)
IT-hydrocortisone dose	.000	-.473						-1.388 (*p*=.177)
IT-hydrocortisone dose * sex	.000	-.390						-.535 (*p*=.597)

IT-hydrocortisone dose * age at diagnosis	.000	.099	.519 (*p*=.608)

B: beta; β: standardized beta; Δ: variation
Online only (supplemental material)

Discussion

Over the past decade, advancements in therapeutic strategies have increased the survival rate of patients with ALL.[63] Despite these improvements, careful monitoring of neurocognitive development is crucial for survivors treated with MTX, as the drug poses a risk of both acute and chronic neurotoxicity.[64] The literature also provides insights into the neurotoxicity associated with cytarabine[65–68] and hydrocortisone[69, 70] in the context of triple IT therapy, as well as other corticosteroids (dexamethasone, prednisolone, and prednisone)[71–73], which can penetrate the blood-brain barrier and access the central nervous system.

This study explored WM integrity, in relation to neurotoxicity risk factors, among adult survivors of pediatric ALL. This study provides further evidence for the idea, well-supported in the existing literature, that the extent of WM microstructural changes is contingent upon the level of exposure to intrathecal MTX.[59, 74] Additionally, this study highlights the dose effects of the other IT agents, cytarabine and hydrocortisone. The cumulative dose of the different IT chemotherapy agents is a factor that aggravates the adverse consequences on the cognitive and cerebral development of children treated for ALL. Moreover, it provides compelling evidence that the mean MTR is a valuable biomarker of long-term neurotoxicity among ALL survivors.

To summarize the key findings of our study, we identified fairly strong negative associations between MTR and dosages of IT agents among long-term survivors of ALL. These

findings suggest that MTR could serve as a sensitive indicator of WM microstructural alterations in this population. Furthermore, lower MTR in the whole brain and CC, along with reduced WM volume fraction, were associated with lower GAI reflecting weaker reasoning abilities. Regression analysis, controlling for relevant factors such as current age, sex, age at diagnosis, and adjunctive cranial radiation therapy (CRT), confirmed the relationship between IT dosages and MTR in both the whole brain and CC. These results highlight the crucial role of MTR as a potential biomarker linking survivors' cognitive complaints with treatment-induced neurotoxicity.

MTR reflects WM tissue composition, especially myelin content, and is sensitive to microstructural changes in myelin. Since in vitro studies, animal models, and post-mortem investigations collectively suggest that chemotherapy-induced neurotoxicity leads to demyelination[75], a decrease in MTR could be indicative of reduced myelination. While MTR can be influenced by various factors, including myelin integrity and axonal density, it is less sensitive to the spatial organization of WM tracts compared to Fractional Anisotropy (FA).[76] FA is a more specific measure of the directionality and coherence of water diffusion along WM tracts, which reflects the spatial organization and alignment of WM fibres.[77] FA has been extensively investigated in ALL survivors, revealing decreased FA values in various regions, including the frontal lobe, the frontostriatal tracts, and the CC.[24, 78] In contrast, very few studies have investigated MTR to detect WM alterations in ALL survivors. Yamamoto and coworkers (2006) observed a decline in peak values within MTR histograms after MTX administration. On the other hand, a more recent study comparing magnetization transfer measures between ALL survivors and healthy controls ended with inconclusive results.[16] To

the best of our knowledge, our study is the first to demonstrate the impact of cumulative doses of chemotherapy agents on MTR means.

In the ongoing quest for a neuroimaging measure sensitive to microstructural damage associated with chemotherapy-induced neurotoxicity, MTR emerges as a promising lead. We raise potential implications for both clinical practice and research. In clinical settings, where treatment-induced neurotoxicity is typically identified through neurological symptoms like seizures, implementing regular follow-up neuroimaging assessments using MTR could offer greatly improved monitoring of neurotoxicity. This heightened surveillance may facilitate earlier detection and enable treatment adjustments to be tailored more precisely according to the child's individual response. In future research endeavors, the integration of MTR in imaging methodology could prove advantageous for exploring the cerebral and cognitive consequences of oncological treatments. Moreover, validation studies will provide valuable insights into the potential clinical implications of our findings and guide the development of more targeted interventions to mitigate neurotoxicity in cancer patients undergoing chemotherapy. The utilization of MTR may represent a compelling avenue for targeting the optimal dosages, aiming to achieve maximum efficacy while minimizing neurotoxicity and its ensuing consequences on the quality of life of cancer survivors.

Turning to another noteworthy observation, the difference in WM volume between ALL survivors and healthy controls did not remain after controlling for intracranial volume. We have not been able to demonstrate in this way a volume loss specific to WM among ALL survivors. However, as in some previous studies[80–82], a group difference was detected in intracranial volume, with survivors exhibiting a smaller intracranial volume compared to the

control group. As the intracranial volume is an index of the global brain volume attained following development, it seems possible that the reduction in intracranial volume reflects somehow the disruption of normal brain development processes in the context of childhood ALL. While a relative loss of WM volume could not be demonstrated, we identified a significant decrease in the mean MTR throughout the whole brain among survivors compared to the control group, and observed a trend in central-to-mid-posterior CC sections.

Our control group was matched for the level of education attained, the age at the time of the study, and sex. A common bias in studies of the neurocognitive status of ALL survivors is the control group which tends to have an average IQ higher than the mean IQ of the normative population (100).[83] Our recruitment efforts have allowed us to form a control group that has an average IQ of 104.9, which does not differ significantly from the normative population mean of 100 ($t(20)=1.622$, $p=.121$). This achievement has contributed to our confidence in presenting the imaging results, as our groups show a considerable level of comparability. With the foregoing in mind, we have observed certain cognitive weaknesses in the group of ALL survivors, highlighting specific cognitive impairments associated with ALL treatments.

Our findings did not provide clear supporting evidence of sex having an impact on the degree of neurocognitive impairment in this cohort of survivors. A trend was observed toward lower MTR means in female compared to male participants, and a significant main effect of sex was found on the mean MTR of the CC. It is plausible that a reduction in MTR impacts women to a greater extent, given their lower MTR values compared to men. However, the present study did not investigate this hypothesis. Yet, evidence suggests that female sex

carries an increased risk of neurocognitive impairment after ALL treatment. Multiple studies have identified sex-related differences in cognitive outcomes, revealing that female survivors tend to exhibit poorer cognitive functioning compared to their male counterparts.[13, 84–86] Congruently, studies indicate a heightened susceptibility to structural and microstructural brain alterations in female survivors.[4, 78, 87, 88] Girls have been shown to exhibit a smaller increase in WM during childhood compared to boys.[89] It is proposed that the variation in WM growth along with hormonal differences may render girls more susceptible to the neurotoxic effects of chemotherapy.[90]

MTX is widely considered the primary culprit, although other agents may also contribute to neurotoxicity.[91] MTX-induced neurotoxicity arises from disruptions in folate physiology and homeostasis, which are vital for neuronal and central nervous system cell function, as they play critical roles in DNA and RNA synthesis, DNA methylation, and maintenance of myelin.[60] More broadly, several mechanisms have been proposed to explain the long-term neurocognitive damages resulting from ALL treatments based on high doses of chemotherapy. There is chemotherapy-induced suppression of cell proliferation, neuroinflammation, the loss of phospholipids affecting white matter architecture and the disturbance of the developing neural networks in the immature brain.[4, 92] Besides, other mechanisms that may have an additive indirect effect on the neurocognitive status of ALL survivors have been raised in the literature. For instance, ALL survivors are at increased risk for chronic cardiopulmonary conditions, which can impact cerebrovascular health by altering cerebral perfusion and blood oxygenation.[93, 94] We are also listing metabolic and endocrine complications such as adrenal insufficiency (compromised hypothalamic-pituitary-adrenal

function), hypogonadism, hypothyroidism, and growth hormone deficiency.[93, 95, 96] Systemic inflammation and oxidative stress are additionally highlighted.[88, 97–100] In future studies exploring the long-term effects of chemotherapy agents on brain integrity and cognition, incorporating metabolic, oxidative, and inflammatory factors would be of great interest.

Limitations should be considered in the interpretation of these results. Firstly, our study had a relatively small sample size, which could have led to the analyses being underpowered. Replicating these findings with a larger cohort of survivors will be informative. Another limitation of our study pertains to the composition of our sample. 27 survivors out of the 35 included in this study received CRT. Of these, all received 18 Gy except one which received 12 Gy. There is evidence to suggest that treatments combining chemotherapy and CRT are associated with greater brain volume loss and WM damage compared to chemotherapy-only treatments.[101–103] CRT is also known to increase the permeability of the blood-brain barrier, which could allow neurotoxic chemotherapy to penetrate the brain more effectively.[104] The combination of CRT and chemotherapy may be associated with greater neurotoxicity.[64] It is therefore possible that the obtained results were influenced by the composition of our sample, with the majority of survivors having received CRT. The generalizability of the results to survivors treated exclusively with chemotherapy is limited and will need to be examined in future studies.

Limitations notwithstanding, our study provides sufficient indications that the MTR can capture the neurotoxic signature of IT treatments almost two decades after pediatric ALL. Our results reveal a decrease in MTR in the whole brain WM and the CC in the adult brain as a

function of the cumulative dose received of the IT agents, MTX, cytarabine and hydrocortisone, during treatments. In conclusion, this study represents a modest yet meaningful step forward in our collective efforts to improve oncological care. By highlighting the potential of MTR as a neurotoxicity indicator, we hope to contribute to the ongoing dialogue surrounding personalized treatment approaches.

References

1. Jeha S, Pei D, Choi J, et al: Improved CNS Control of Childhood Acute Lymphoblastic Leukemia Without Cranial Irradiation: St Jude Total Therapy Study 16 [Internet]. Journal of Clinical Oncology 37:3377, 2019[cited 2022 Oct 13] Available from: /pmc/articles/PMC7351342/

2. Waber DP, Turek J, Catania L, et al: Neuropsychological outcomes from a randomized trial of triple intrathecal chemotherapy compared with 18 Gy cranial radiation as CNS treatment in acute lymphoblastic leukemia: Findings from Dana-Farber Cancer Institute ALL Consortium Protocol 95-01. Journal of Clinical Oncology 25:4914–4921, 2007

3. Vora A, Andreano A, Pui CH, et al: Influence of Cranial Radiotherapy on Outcome in Children With Acute Lymphoblastic Leukemia Treated With Contemporary Therapy [Internet]. Journal of Clinical Oncology 34:919, 2016[cited 2022 Oct 13] Available from: /pmc/articles/PMC4871998/

4. Reddick WE, Taghipour DJ, Glass JO, et al: Prognostic factors that increase the risk for reduced white matter volumes and deficits in attention and learning for survivors of childhood cancers [Internet]. Pediatr Blood Cancer 61:1074–1079, 2014[cited 2022 Sep 25] Available from: https://onlinelibrary.wiley.com/doi/full/10.1002/pbc.24947

5. Boulet-Craig A, Robaey P, Laniel J, et al: DIVERGT screening procedure predicts general cognitive functioning in adult long-term survivors of pediatric acute lymphoblastic leukemia: A PETALE study [Internet]. Pediatr Blood Cancer 65, 2018[cited 2021 Nov 8] Available from: https://pubmed.ncbi.nlm.nih.gov/29797640/

6. Krull KR, Brinkman TM, Li C, et al: Neurocognitive outcomes decades after treatment for childhood acute lymphoblastic leukemia: A report from the St jude lifetime cohort study. Journal of Clinical Oncology 31:4407–4415, 2013

7. Krull KR, Brinkman TM, Li C, et al: Neurocognitive outcomes decades after treatment for childhood acute lymphoblastic leukemia: A report from the St jude lifetime cohort study. Journal of Clinical Oncology 31:4407–4415, 2013

8. Waber DP, Mccabe M, Sebree M, et al: Neuropsychological outcomes of a randomized trial of prednisone versus dexamethasone in acute lymphoblastic leukemia: Findings from dana-farber cancer institute all consortium protocol 00-01. Pediatr Blood Cancer 60:1785–1791, 2013

9. Darling SJ, de Luca C, Anderson V, et al: White Matter Microstructure and Information Processing at the Completion of Chemotherapy-Only Treatment for Pediatric Acute Lymphoblastic Leukemia. Dev Neuropsychol 43:385–402, 2018

10. Zeller B, Tamnes CK, Kanellopoulos A, et al: Reduced neuroanatomic volumes in long-term survivors of childhood acute lymphoblastic leukemia. Journal of Clinical Oncology 31:2078–2085, 2013

11. Genschaft M, Huebner T, Plessow F, et al: Impact of chemotherapy for childhood leukemia on brain morphology and function. PLoS One 8, 2013

12. Armstrong GT, Sklar CA, Hudson MM, et al: Long-term health status among survivors of childhood cancer: does sex matter? [Internet]. J Clin Oncol 25:4477–4489, 2007[cited 2023 Jun 14] Available from: https://pubmed.ncbi.nlm.nih.gov/17906209/

13. Buizer AI, De Sonneville LMJ, Veerman AJP: Effects of chemotherapy on neurocognitive function in children with acute lymphoblastic leukemia: A critical review of the literature [Internet]. Pediatr Blood Cancer 52:447–454, 2009[cited 2023 Jun 7] Available from: https://onlinelibrary.wiley.com/doi/full/10.1002/pbc.21869

14. Cheung YT, Krull KR: Neurocognitive outcomes in long-term survivors of childhood acute lymphoblastic leukemia treated on contemporary treatment protocols: A systematic review [Internet]. Neurosci Biobehav Rev 53:108–120, 2015Available from: http://dx.doi.org/10.1016/j.neubiorev.2015.03.016

15. Waber DP, Queally JT, Catania L, et al: Neuropsychological outcomes of standard risk and high risk patients treated for acute lymphoblastic leukemia on Dana-Farber ALL consortium protocol 95-01 at 5 years post-diagnosis. Pediatr Blood Cancer 58:758–765, 2012
16. van der Plas E, Schachar RJ, Hitzler J, et al: Brain structure, working memory and response inhibition in childhood leukemia survivors [Internet]. Brain Behav 7, 2017[cited 2022 Apr 24] Available from: /pmc/articles/PMC5318374/
17. Merriman JD, Von Ah D, Miaskowski C, et al: Proposed Mechanisms for Cancer- and Treatment-Related Cognitive Changes. Semin Oncol Nurs 29:260–269, 2013
18. Kesler SR, Rao A, Blayney DW, et al: Predicting long-term cognitive outcome following breast cancer with pre-treatment resting state fMRI and random forest machine learning [Internet]. Front Hum Neurosci 11, 2017[cited 2023 Aug 8] Available from: /pmc/articles/PMC5694825/
19. Zhou C, Zhuang Y, Lin X, et al: Changes in neurocognitive function and central nervous system structure in childhood acute lymphoblastic leukaemia survivors after treatment: a meta-analysis. Br J Haematol 188:945–961, 2020
20. Aukema EJ, Caan MWA, Oudhuis N, et al: White Matter Fractional Anisotropy Correlates With Speed of Processing and Motor Speed in Young Childhood Cancer Survivors. Int J Radiat Oncol Biol Phys 74:837–843, 2009
21. Voon NS, Manan HA, Yahya N: Diffusion tensor imaging indices as biomarkers for cognitive changes following paediatric radiotherapy: a systematic review and meta-analysis [Internet]. Strahlentherapie und Onkologie 198:409–426, 2022[cited 2023 Jun 20] Available from: https://link.springer.com/article/10.1007/s00066-022-01905-6
22. Sabin ND, Cheung YT, Reddick WE, et al: The Impact of Persistent Leukoencephalopathy on Brain White Matter Microstructure in Long-Term Survivors of Acute Lymphoblastic Leukemia Treated with Chemotherapy Only [Internet]. AJNR Am J Neuroradiol 39:1919–1925, 2018[cited 2023 Jun 7] Available from: https://pubmed.ncbi.nlm.nih.gov/30213807/
23. Kesler SR, Tanaka H, Koovakkattu D: Cognitive reserve and brain volumes in pediatric acute lymphoblastic leukemia. Brain Imaging Behav 4:256–269, 2010

24. Wei K, Liang Y, Yang B, et al: An observational MRI study of methotrexate-treated children with acute lymphoblastic leukemia in remission and subtle cognitive decline [Internet]. Quant Imaging Med Surg 12:2474–2486, 2022[cited 2023 Jun 7] Available from: https://dx.doi.org/10.21037/qims-21-748

25. Marcoux S, Drouin S, Laverdière C, et al: The PETALE study: Late adverse effects and biomarkers in childhood acute lymphoblastic leukemia survivors. Pediatr Blood Cancer 64, 2017

26. Krull KR, Okcu MF, Potter B, et al: Screening for neurocognitive impairment in pediatric cancer long-term survivors [Internet]. Journal of Clinical Oncology 26:4138–4143, 2008[cited 2021 Nov 8] Available from: https://pubmed.ncbi.nlm.nih.gov/18757327/

27. Boulet-Craig A, Robaey P, Barlaam F, et al: Visual Short-Term Memory Activation Patterns in Adult Survivors of Childhood Acute Lymphoblastic Leukemia. Cancer October 15, 2019

28. Cabana J-F, Gu YE, Boudreau M, et al: Quantitative Magnetization Transfer Imaging Made Easy with qMTLab: Software for Data Simulation, Analysis, and Visualization. Concepts in Magnetic Resonance Part A 44A:263–277, 2015

29. Fischl B: FreeSurfer. Neuroimage 62:774–781, 2012

30. Ségonne F, Dale AM, Busa E, et al: A hybrid approach to the skull stripping problem in MRI [Internet]. Neuroimage 22:1060–1075, 2004Available from: www.sciencedirect.com.

31. Fischl B, Salat DH, Busa E, et al: Neurotechnique Whole Brain Segmentation: Automated Labeling of Neuroanatomical Structures in the Human Brain. Neurotechnique 33:341–355, 2002

32. Sled J, Zijdenbos A, Evans A: A nonparametric method for automatic correction of intensity nonuniformity in MRI data [Internet]. IEEE Trans Med Imaging 17:87–97, 1998[cited 2021 Oct 19] Available from: https://pubmed.ncbi.nlm.nih.gov/9617910/

33. Ségonne F, Pacheco J, Fischl B: Geometrically accurate topology-correction of cortical surfaces using nonseparating loops [Internet]. IEEE Trans Med Imaging 26:518–529, 2007[cited 2021 Oct 19] Available from: https://pubmed.ncbi.nlm.nih.gov/17427739/

34. Buckner RL, Head D, Parker J, et al: A unified approach for morphometric and functional data analysis in young, old, and demented adults using automated atlas-based head size

normalization: reliability and validation against manual measurement of total intracranial volume. Neuroimage 23:724–738, 2004

35. Jenkinson M, Bannister P, Brady M, et al: Improved Optimization for the Robust and Accurate Linear Registration and Motion Correction of Brain Images, 2002

36. Wechsler D: Wechsler Adult Intelligence Scale 4th ed. NCS Pearson , 2008

37. Delis D, Kaplan E, Kramer J: Delis–Kaplan Executive Function System. Psychological Corporation , 2001

38. Klove H: Grooved Pegboard Test. Lafayette Instrument Company , 1963

39. Cohen J: A Power Primer. Psychol Bull 112:155–159, 1992

40. Cohen J: Statistical power analysis for the behavioral sciences. Academic press , 2013

41. Benjamini Y, Hochberg Y: Controlling the False Discovery Rate: a Practical and Powerful Approach to Multiple Testing. Journal of the Royal Statistical Society: Series B 57:289–300, 1995

42. Benjamini Y, Yekutieli D: The Control of the False Discovery Rate in Multiple Testing under Dependency. The Annals of Statistics 29:1165–1188, 2001

43. Glickman ME, Rao SR, Schultz MR: False discovery rate control is a recommended alternative to Bonferroni-type adjustments in health studies. J Clin Epidemiol 67:850–857, 2014

44. Streiner DL, Norman GR: Correction for Multiple Testing: Is There a Resolution? Chest 140:16–18, 2011

45. Baynes K: Corpus Callosum, in Encyclopedia of the Human Brain Academic Press. 2002, pp 51–64

46. Eccher M: Corpus Callosum, in Encyclopedia of the Neurological Sciences. Academic Press, 2014, pp 867–868

47. Bartha-Doering L, Kollndorfer K, Schwartz E, et al: The role of the corpus callosum in language network connectivity in children. Dev Sci 24, 2021

48. Koch K, Wagner G, Schachtzabel C, et al: Age-dependent visuomotor performance and white matter structure: a DTI study. Brain Struct Funct 218:1075–1084, 2013

49. Degraeve B, Sequeira H, Mecheri H, et al: Corpus callosum damage to account for cognitive, affective, and social-cognitive dysfunctions in multiple sclerosis: A model of callosal disconnection syndrome? Multiple Sclerosis Journal 29:160–168, 2023
50. Llufriu S, Blanco Y, Martinez-Heras E, et al: Influence of Corpus Callosum Damage on Cognition and Physical Disability in Multiple Sclerosis: A Multimodal Study [Internet]. PLoS One 7, 2012[cited 2023 Jul 9] Available from: www.plosone.org
51. Pfefferbaum A, Adalsteinsson E, Sullivan E V: Dysmorphology and microstructural degradation of the corpus callosum: Interaction of age and alcoholism. Neurobiol Aging 27:994–1009, 2006
52. Luders E, Toga AW: Sex differences in brain anatomy. Prog Brain Res 186:2–12, 2010
53. Lüders E, Steinmetz H, Jäncke L: Brain size and grey matter volume in the healthy human brain [Internet]. Neuroreport 13:2371–2374, 2002[cited 2023 Jul 18] Available from: https://pubmed.ncbi.nlm.nih.gov/12488829/
54. Eikenes L, Visser E, Vangberg T, et al: Both brain size and biological sex contribute to variation in white matter microstructure in middle-aged healthy adults. Hum Brain Mapp 44:691–709, 2023
55. Björnholm L, Nikkinen J, Kiviniemi V, et al: Structural properties of the human corpus callosum: Multimodal assessment and sex differences [Internet]. Neuroimage 152:108–118, 2017[cited 2023 Jul 1] Available from: http://dx.doi.org/10.1016/j.neuroimage.2017.02.056
56. Silver NC, Barker GJ, MacManus DG, et al: Magnetisation transfer ratio of normal brain white matter: a normative database spanning four decades of life. [Internet]. J Neurol Neurosurg Psychiatry 62:223–228, 1997[cited 2023 Jul 18] Available from: https://jnnp.bmj.com/content/62/3/223
57. Armstrong CL, Traipe E, Hunter J V, et al: Age-Related, Regional, Hemispheric, and Medial-Lateral Differences in Myelin Integrity in Vivo in the Normal Adult Brain. American journal of neuroradiology 25, 2004
58. Iyer NS, Balsamo LM, Bracken MB, et al: Chemotherapy-only treatment effects on long-term neurocognitive functioning in childhood ALL survivors: A review and meta-analysis. Blood 126:346–353, 2015

59. Krull KR, Cheung YT, Liu W, et al: Chemotherapy pharmacodynamics and neuroimaging and neurocognitive outcomes in long-term survivors of childhood acute lymphoblastic leukemia. Journal of Clinical Oncology 34:2644–2653, 2016
60. Bhojwani D, Sabin ND, Pei D, et al: Methotrexate-induced neurotoxicity and leukoencephalopathy in childhood acute lymphoblastic leukemia. Journal of Clinical Oncology 32:949–959, 2014
61. Azhideh A, Taherian M, Tajabadi Z, et al: Methotrexate-induced neurocognitive late effects in treatment of pediatric acute lymphoblastic leukemia: a review [Internet]. Journal of Human, Health and Halal Metrics 2:63–74, 2021Available from: https://doi.org/10.30502/jhhhm.2021.283539.1031
62. Śliwa-Tytko P, Kaczmarska A, Lejman M, et al: Neurotoxicity Associated with Treatment of Acute Lymphoblastic Leukemia Chemotherapy and Immunotherapy [Internet]. Int J Mol Sci 23, 2022[cited 2023 May 3] Available from: /pmc/articles/PMC9146746/
63. Richards S, Pui CH, Gayon P: Systematic Review and Meta-analysis of Randomized Trials of Central Nervous System Directed Therapy for Childhood Acute Lymphoblastic Leukaemia [Internet]. Pediatr Blood Cancer 60:185, 2013[cited 2023 Jul 19] Available from: /pmc/articles/PMC3461084/
64. Cole PD, Kamen BA: Delayed neurotoxicity associated with therapy for children with acute lymphoblastic leukemia. Ment Retard Dev Disabil Res Rev 12:174–183, 2006
65. Takahashi S, Sato S, Igarashi S, et al: Neurocognitive deficits in survivors of childhood acute myeloid leukemia [Internet]. BMC Pediatr 22:1–8, 2022[cited 2023 Jul 19] Available from: https://bmcpediatr.biomedcentral.com/articles/10.1186/s12887-022-03369-0
66. Herzig RH, Hines JD, Herzig GP, et al: Cerebellar toxicity with high-dose cytosine arabinoside. Journal of Clinical Oncology 5:927–932, 1987
67. Kerr JZ, Berg S, Blaney SM: Intrathecal chemotherapy. Crit Rev Oncol Hematol 37:227–236, 2001
68. Bassan R, Masciulli A, Intermesoli T, et al: Randomized trial of radiation-free central nervous system prophylaxis comparing intrathecal triple therapy with liposomal cytarabine in

acute lymphoblastic leukemia [Internet]. Haematologica 100:786, 2015[cited 2023 Jul 19] Available from: /pmc/articles/PMC4450624/

69. Kadan-Lottick NS, Brouwers P, Breiger D, et al: Comparison of neurocognitive functioning in children previously randomly assigned to intrathecal methotrexate compared with triple intrathecal therapy for the treatment of childhood acute lymphoblastic leukemia [Internet]. J Clin Oncol 27:5986–5992, 2009[cited 2023 Jul 19] Available from: https://pubmed.ncbi.nlm.nih.gov/19884541/

70. ElAlfy M, Ragab I, Azab I, et al: Neurocognitive Outcome and White Matter Anisotropy in Childhood Acute Lymphoblastic Leukemia Survivors Treated with Different Protocols [Internet]. Pediatr Hematol Oncol 31:194–204, 2014[cited 2023 Jul 19] Available from: https://www.tandfonline.com/action/journalInformation?journalCode=ipho20

71. Hardy KK, Embry L, Kairalla JA, et al: Neurocognitive Functioning of Children Treated for High-Risk B-Acute Lymphoblastic Leukemia Randomly Assigned to Different Methotrexate and Corticosteroid Treatment Strategies: A Report From the Children's Oncology Group [Internet]. Journal of Clinical Oncology 35:2700–2707, 2017Available from: https://doi.org/10.1200/JCO.2016.

72. Aminath S, Dhillon G, Latheef S, et al: Study of exposure to dexamethasone among children with acute lymphoblastic leukemia and effect on intellectual function – A pilot study. Current Medical Issues 19:144, 2021

73. Phillips NS, Ting Cheung Y, Glass JO, et al: Neuroanatomical abnormalities related to dexamethasone exposure in survivors of childhood acute lymphoblastic leukemia [Internet]. Pediatr Blood Cancer 67, 2020[cited 2023 Jun 7] Available from: https://onlinelibrary.wiley.com/doi/10.1002/pbc.27968

74. Kesler SR, Sleurs C, McDonald BC, et al: Brain Imaging in Pediatric Cancer Survivors: Correlates of Cognitive Impairment [Internet]. Journal of Clinical Oncology 39:1775–1785, 2021[cited 2021 Nov 17] Available from: https://oce.ovid.com/article/00005083-202106010-00009/HTML

75. Deprez S, Billiet T, Sunaert S, et al: Diffusion tensor MRI of chemotherapy-induced cognitive impairment in non-CNS cancer patients: A review [Internet]. Brain Imaging Behav

7:409–435, 2013[cited 2023 Jul 1] Available from: https://link.springer.com/article/10.1007/s11682-012-9220-1

76. Schmierer K, Scaravilli F, Altmann DR, et al: Magnetization transfer ratio and myelin in postmortem multiple sclerosis brain [Internet]. Ann Neurol 56:407–415, 2004[cited 2023 Jul 19] Available from: https://onlinelibrary.wiley.com/doi/full/10.1002/ana.20202

77. Stikov N, Perry LM, Mezer A, et al: Bound Pool Fractions Complement Diffusion Measures to Describe White Matter Micro and Macrostructure [Internet]. Neuroimage 54:1112, 2011[cited 2023 Jul 19] Available from: /pmc/articles/PMC2997845/

78. Gandy K, Scoggins MA, Jacola LM, et al: Structural and Functional Brain Imaging in Long-Term Survivors of Childhood Acute Lymphoblastic Leukemia Treated With Chemotherapy: A Systematic Review [Internet]. JNCI Cancer Spectr 5, 2021[cited 2022 Aug 18] Available from: https://pubmed.ncbi.nlm.nih.gov/34514328/

79. Yamamoto A, Miki Y, Adachi S, et al: Whole brain magnetization transfer histogram analysis of pediatric acute lymphoblastic leukemia patients receiving intrathecal methotrexate therapy. Eur J Radiol 57:423–427, 2006

80. van der Plas E, Spencer Noakes TL, Butcher DT, et al: Quantitative MRI outcomes in child and adolescent leukemia survivors: Evidence for global alterations in gray and white matter. Neuroimage Clin 28, 2020

81. Zeller B, Tamnes CK, Kanellopoulos A, et al: Reduced neuroanatomic volumes in long-term survivors of childhood acute lymphoblastic leukemia. Journal of Clinical Oncology 31:2078–2085, 2013

82. Follin C, Gabery S, Petersén Å, et al: Associations between Metabolic Risk Factors and the Hypothalamic Volume in Childhood Leukemia Survivors Treated with Cranial Radiotherapy. PLoS One 11:147575, 2016

83. Cao SC, Legerstee JS, van Bellinghen M, et al: Effect of chemotherapy (with and without radiotherapy) on the intelligence of children and adolescents treated for acute lymphoblastic leukemia; a meta-analysis. Psychooncology , 2023

84. Janzen LA, Spiegler BJ: Neurodevelopmental sequelae of pediatric acute lymphoblastic leukemia and its treatment [Internet]. Dev Disabil Res Rev 14:185–195, 2008[cited 2023 Jul 19] Available from: https://onlinelibrary.wiley.com/doi/10.1002/ddrr.24

85. Partanen M, Phipps S, Russell K, et al: Longitudinal Trajectories of Neurocognitive Functioning in Childhood Acute Lymphoblastic Leukemia [Internet]. J Pediatr Psychol 46:168–178, 2021[cited 2023 Jul 19] Available from: https://academic.oup.com/jpepsy/article/46/2/168/5917812

86. Jacola LM, Krull KR, Pui CH, et al: Longitudinal assessment of neurocognitive outcomes in survivors of childhood acute lymphoblastic leukemia treated on a contemporary chemotherapy protocol. Journal of Clinical Oncology 34:1239–1247, 2016

87. Phillips NS, Cheung YT, Glass JO, et al: Neuroanatomical abnormalities related to dexamethasone exposure in survivors of childhood acute lymphoblastic leukemia. Pediatr Blood Cancer 67, 2020

88. Phillips NS, Kesler SR, Scoggins MA, et al: Connectivity of the Cerebello-Thalamo-Cortical Pathway in Survivors of Childhood Leukemia Treated With Chemotherapy Only [Internet]. JAMA Netw Open 3, 2020[cited 2023 Jun 20] Available from: /pmc/articles/PMC7679952/

89. De Bellis MD, Keshavan MS, Beers SR, et al: Sex differences in brain maturation during childhood and adolescence [Internet]. Cerebral cortex 11:552–557, 2001[cited 2023 Jun 7] Available from: https://pubmed.ncbi.nlm.nih.gov/11375916/

90. van der Plas E, Qiu W, Nieman BJ, et al: Sex-Specific Associations Between Chemotherapy, Chronic Conditions, and Neurocognitive Impairment in Acute Lymphoblastic Leukemia Survivors: A Report From the Childhood Cancer Survivor Study [Internet]. J Natl Cancer Inst 113:588–596, 2021[cited 2023 Jun 7] Available from: https://academic.oup.com/jnci/article/113/5/588/5901053

91. Thastrup M, Duguid A, Mirian C, et al: Central nervous system involvement in childhood acute lymphoblastic leukemia: challenges and solutions [Internet]. Leukemia 36:2751–2768, 2022[cited 2023 Jun 24] Available from: https://doi.org/10.1038/s41375-022-01714-x

92. Al-Mahayri ZN, AlAhmad MM, Ali BR: Long-Term Effects of Pediatric Acute Lymphoblastic Leukemia Chemotherapy: Can Recent Findings Inform Old Strategies? Front Oncol 11, 2021

93. Cheung YT, Brinkman TM, Li C, et al: Chronic Health Conditions and Neurocognitive Function in Aging Survivors of Childhood Cancer: A Report from the Childhood Cancer Survivor Study [Internet]. JNCI Journal of the National Cancer Institute 110:411, 2018[cited 2023 Jun 11] Available from: /pmc/articles/PMC6059140/

94. Williams AM, Cheung YT, Hyun G, et al: Childhood Neurotoxicity and Brain Resilience to Adverse Events during Adulthood [Internet]. Ann Neurol 89:534–545, 2020[cited 2023 Jun 15] Available from: https://onlinelibrary.wiley.com/doi/10.1002/ana.25981

95. Cheung YT, Chemaitilly W, Mulrooney DA, et al: Association between Dehydroepiandrosterone-sulfate and Attention in Long-term Survivors of Childhood Acute Lymphoblastic Leukemia Treated with Only Chemotherapy [Internet]. Psychoneuroendocrinology 76:114, 2017[cited 2023 Jun 14] Available from: /pmc/articles/PMC5272831/

96. Phillips NS, Stratton KL, Williams AM, et al: Late-onset Cognitive Impairment and Modifiable Risk Factors in Adult Childhood Cancer Survivors [Internet]. JAMA Netw Open 6:e2316077, 2023[cited 2023 Jun 15] Available from: /pmc/articles/PMC10233416/

97. Cheung YT, Brinkman TM, Mulrooney DA, et al: Impact of Sleep, Fatigue and Systemic Inflammation on Neurocognitive and Behavioral Outcomes in Long-term Survivors of Childhood Acute Lymphoblastic Leukemia [Internet]. Cancer 123:3410, 2017[cited 2023 Jun 14] Available from: /pmc/articles/PMC5570612/

98. Rossi F, Di Paola A, Pota E, et al: Biological aspects of inflamm-aging in childhood cancer survivors. Cancers (Basel) 13, 2021

99. Gupta P, Kaur Makkar T, Goel L, et al: Role of inflammation and oxidative stress in chemotherapy-induced neurotoxicity [Internet]. Immunol Res 70:725–741, 2022[cited 2023 Jul 19] Available from: https://doi.org/10.1007/s12026-022-09307-7

100. Léveillé P, Boulet-Craig A, Laniel J, et al: Complications cardiométaboliques et déficits cognitifs chez les survivants de la leucémie lymphoblastique aiguë pédiatrique : associations avec l'inflammation périphérique ? Nutrition Clinique et Métabolisme 33:67, 2019

101. Reddick WE, Shan ZY, Glass JO, et al: Smaller white-matter volumes are associated with larger deficits in attention and learning among long-term survivors of acute lymphoblastic leukemia. Cancer 106:941–949, 2006

102. Zając-Spychała O, Pawlak M, Karmelita-Katulska K, et al: Anti-leukemic treatment-induced neurotoxicity in long-term survivors of childhood acute lymphoblastic leukemia: impact of reduced central nervous system radiotherapy and intermediate- to high-dose methotrexate. Leuk Lymphoma 59:2342–2351, 2018

103. Reddick WE, Laningham FH, Glass JO, et al: Quantitative morphologic evaluation of magnetic resonance imaging during and after treatment of childhood leukemia [Internet]. Neuroradiology 49:889–904, 2007[cited 2023 Jun 24] Available from: http://www.stjude.org/reddick

104. Hart E, Odé Z, Derieppe MPP, et al: Blood-brain barrier permeability following conventional photon radiotherapy – A systematic review and meta-analysis of clinical and preclinical studies [Internet]. Clin Transl Radiat Oncol 35:44, 2022[cited 2023 Jun 11] Available from: /pmc/articles/PMC9117815/